# REMOTE ACOUSTIC MATERIAL CHARACTERIZATION OF THIN SHEETS

Etienne Marcelin Mfoumou

Blekinge Institute of Technology
Licentiate Dissertation Series No. 2006:09

School of Engineering

# Remote Acoustic Material Characterization of Thin Sheets

Etienne Marcelin Mfoumou

Blekinge Institute of Technology Licentiate Dissertation Series
No 2006:09
ISSN 1650-2140
ISBN 91-7295-094-3

# Remote Acoustic Material Characterization of Thin Sheets

**Etienne Marcelin Mfoumou**


School of Engineering
Blekinge Institute of Technology
SWEDEN

School of Engineering
Publisher: Blekinge Institute of Technology
Printed by Kaserntryckeriet, Karlskrona, Sweden 2006
ISBN 91-7295-094-3

# Acknowledgments

This work was carried out at the Department of Mechanical Engineering, School of Engineering, Blekinge Institute of Technology (BTH), Karlskrona, Sweden, under the supervision of Associate Professor Claes Hedberg and PhD Sharon Kao-Walter.

First and foremost, I would like to express my gratitude to my supervisors, as well as to Prof. O. V. Rudenko, for sharing their interesting ideas, knowledge and experiences, and for supporting me throughout this work.

I would also like to thank my colleague Kristian Haller for assisting me in experimental setup.

Finally, I am grateful for the financial support during my research studies from the Faculty Board of Blekinge Institute of Technology, Sweden. My thanks are also addressed to the Department of Mechanical Engineering / ENSET of the University of Douala in Cameroon.

Karlskrona, November 2006
Etienne M. Mfoumou

# Abstract

There is a need to monitor the existence and effects of damage in structural materials. Aircraft components provide a much publicized example, but the need exists in a variety of other structures, such as layered materials used in food packaging industries. While several techniques and models have been proposed for material characterization and condition monitoring of bulk materials, less attention has been devoted to thin sheets having no flexural rigidity. This study is therefore devoted to the development of a new method for acoustic Non-Destructive Testing (NDT) and material characterization of thin sheets used in food packaging materials or similar structures.

A method for assessing the strength in the presence of crack of thin sheets used in food packaging is first presented using a modified Strip Yield Model (SYM). Resonance frequency measurement is then introduced and it is shown, at low frequency range (less than 2kHz), that a change in the physical properties such as a reduction in stiffness resulting from the onset of cracks or loosening of a connection causes detectable changes in the modal properties, specifically the resonance frequency. This observation leads to the implementation of a simple method for damage severity assessment on sheet materials, supported by a new theory illustrating the feasibility of the detection of inhomogeneity in form of added mass, as well as damage severity assessment, using a measurement of the frequency shift. A relationship is then established between the resonance frequency and the material's elastic property, which yields a new modality for sheet materials remote characterization.

The result of this study is the groundwork of a low-frequency vibration-based method with remote acoustic excitation and laser detection, for non-

destructive testing and material characterization of sheet materials. The work also enhances the feasibility of the testing and condition monitoring of real structures in their operating environment, rather than laboratory tests of representative structures. The sensitivity of the new experimental approach used is liable to improvement while being high because the frequency measurement is one of the most accurate measurements in physics and metrology.

**Keywords:** Remote acoustic excitation, material characterization, acoustic NDT, vibration-based technique, sheet material evaluation, fracture toughness.

# Thesis

### Disposition

This thesis includes an introductory part and the following appended papers:

**Paper A**

Mfoumou, E., Kao-Walter, S., and Hedberg, C., *Fracture Mechanism and Acoustic Damage Analysis of Thin Materials*, pp 1248 in Proc. Of the 11th International Conference on Fracture, Turin, Italy (2005).

**Paper B**

Mfoumou, E., Hedberg, C., and Kao-Walter, S., *Vibration-based for Damage Detection and Evaluation of Sheet Materials using a Remote Acoustic Excitation.* Manuscript in review for journal publication (2006).

**Paper C**

Mfoumou, E., Rudenko, O.V., Hedberg, C., and Kao-Walter, S., *Acoustical Measurement Accompanying Tensile Test: New Modality for Non-Destructive Testing and Characterization of Sheet Materials.* CD-ROM Proceedings of the 13th International Congress on Sound and Vibration (ICSV13), July 2-6, 2006, Vienna, Austria, Eds.: Eberhardsteiner, J.; Mang, H.A.; Waubke, H., Publisher: Vienna University of Technology, Austria, ISBN: 3-9501554-5-7

**Paper D**

Mfoumou, E., Rudenko, O.V., Hedberg, C., and Kao-Walter, S., *Static versus Low Frequency Dynamic Elastic Modulus Measurement of Thin Films.* Accepted for publication in the journal *Technical Acoustics* (2006).

### The Author's Contribution to the Papers

The appended papers are prepared in collaboration with co-authors. The present author's contributions are as follows:

**Paper A**
Took part in the planning of the paper and performed the experiments. Wrote the paper together with co-authors.

**Paper B**
Performed the experiments and the finite element analysis. The paper was written jointly by all authors.

**Paper C**
Initiated the work and performed the experiments. Took part in the calculations and discussions during the working process. Wrote the paper together with co-authors.

**Paper D**
Initiated the work and performed the experiments together with Kao-Walter. Wrote the paper together with co-authors.

# Contents

# Chapter 1

# Introduction

## 1.1 Background

The interest in the ability to monitor a structure and detect damage at the earliest possible stage is pervasive throughout the civil, mechanical, and aerospace engineering communities. For the purpose of our investigation, damage is defined as changes introduced into the material, either intentional or unintentional, which adversely affect the current or future performance of the system. However, depending on the levels of exposure, the system may not show the negative effects of the damaging event for many years or even future generations. Implicit in this definition of damage is that the concept of damage is not meaningful without a comparison between two different states of the system, one of which is assumed to represent the initial, and often undamaged, state.

Most currently used damage identification methods are included in one of the following categories: visual or localized experimental methods such as acoustic or ultrasonic methods, magnetic field methods, radiography, eddy-current methods or thermal field methods [1]. All of these experimental techniques require that the vicinity of the damage is known a priori and that the portion of the structure being inspected is readily accessible. However, in the last few years, new interesting aspects have drawn up the interest in the so-called *Nonlinear Non-Destructive Testing* (NNDT), and a review of some experimental results on material characterization is given in reference [2]. In

the same line of investigation, Hedberg et al. [3] studied the feasibility of the remote evaluation and testing of a layer by interpreting its acoustic signals scattered by a linear or nonlinear inhomogeneity. The outcome from that work is the groundwork for the qualitative analysis of more complicated scatterers and structures [4]. In parallel, the need for quantitative global damage detection methods that can be applied to complex structures (in shape and size) has motivated the development and continued research of methods that examine changes in the vibration characteristics of the structure [5–9]. Meanwhile, the increase in research activity regarding vibration-based condition monitoring is the result of the coupling between many factors. These factors include spectacular failures resulting in loss of life that have received ample news media coverage, economic concerns, and recent technical advancements.

Damage or fault detection, as determined by changes in the dynamic properties or response of systems, has always been practiced in a qualitative manner, using acoustic techniques. More recently, this subject has received considerable attention in the technical literature where there has been a concerted effort to develop a firmer mathematical and physical foundation for this technology [10–12]. This work is one of the first in the field dealing with thin materials with thickness of the order of microns at low frequency range. It also stands for a contribution to the engineering community in launching a method of low frequency vibration-based from a remote acoustic excitation as a possible measurement for nondestructive evaluation of materials (see Figure 1.1). However, the basic idea remains that the measured resonance frequencies are functions of the physical properties of the structure, specifically the mass and the stiffness. Therefore, changes in the physical properties allow monitoring the resonance frequency. Inversely, the resonance frequency measurement can be used as a technique for material characterization.

Meanwhile, an acoustic method is already well-known in the Fracture Mechanics community as an efficient technique for the fracture toughness measurement under static loading conditions. The technique uses the acoustic emission to monitor real-time crack initiation and propagation around the principal crack [13–15]. This is not suitable for contact sensitive materials

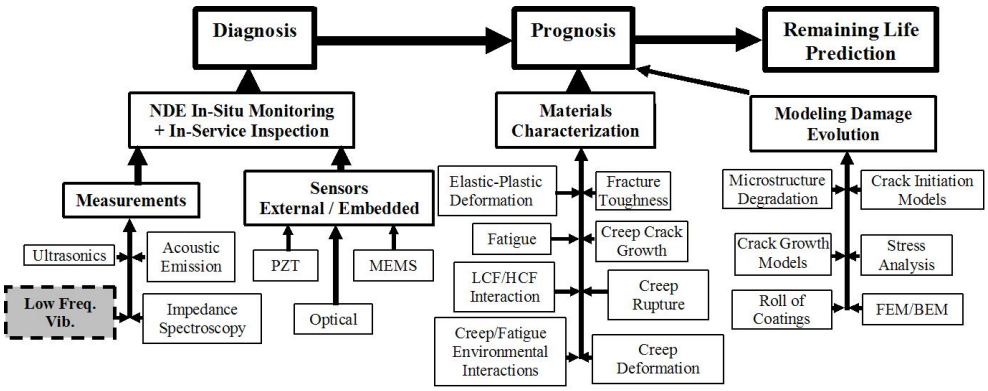


Figure 1.1: The contribution to the engineering community is the new shaded measurement technique box

such as those used in food packages, motivating the implementation of a new acoustic technique based on a remote evaluation of the material.

It has also been shown quite recently that elastic nonlinearity of imperfect materials strongly depends on super-molecular structures like voids, micro-cracks, grain boundaries, and others [2, 16]. This observation may apply to thin sheets, and these molecular structures can be easily detected by means of nonlinear acoustic methods. This leads to a challenging opportunity of linear and nonlinear characterization of structural changes of materials and constructions by monitoring their mechanical properties in manufacturing and service, which is the step for which this thesis constitutes the groundwork.

Thin sheets constitute a class of engineering materials with application areas expanding with the continuous engineering process. The casting of paper from wood-pulps, the rolling of metallic foils, and the forming of polymer films and some of the composites layered structures are examples of such processes. The motion of the material in its manufacturing process as well as the in-situ investigation of the material integrity requires a non-destructive technique. Besides, a remote investigation may be necessary at high temperatures for instance for corrosive materials when the direct contact between the transducer and the material under study is impossible, or in case of investigation of contact-sensitive materials such as those under investigation in this thesis.

It may sometimes be desirable to detect a small imperfection in the shortest possible time.

## 1.2 Problem description

Imperfections of sheet materials have very different structures. They can be formed by sheet sections the thickness of which some are greater or smaller than the targeted tolerance. Voids, cracks and zones of reduced strength can appear inside the material. For composite packaging materials used in the food industry (and containing, for example, layers of water-repellent cardboard, polyethylene, aluminum foil) the important problem is in the detection of both delaminated areas and the damages of internal layers at bends, breaking the impermeability of the food package and leading to the fermentation of the foodstuff, making it useless [17].

Moreover, residual stresses in and between the layers of a laminate develop during processing and arise from a combination of mismatched thermal expansion coefficients and intermolecular forces. These residual stresses increase the probability of stress-related failures due to mechanisms such as electromigration, stress migration, and delamination [18]. This yields the need of an unavoidable efficient technique for the materials characterization, and the acoustic emission already used for the fracture toughness measurement is well-suited for thin flexible materials having no (or negligible) bending stiffness.

## 1.3 Aim and scope

The present research is focused on the implementation of an effective non-destructive evaluation technique based on dynamic characterization for the purpose of evaluating the relationship between changes in the vibration frequencies of thin sheets and different levels of damage. The aim of this study is then to detect damage and determine mechanical properties of thin sheets by means of a simple remote acoustic measurement. The work is also a gateway for a non-contact monitoring of a real-time crack initiation and propagation

for the fracture toughness measurement. To achieve our goal, the method of measuring the resonance frequencies of the structure from a remote acoustic excitation is used, which is comparatively new in the area of non-destructive testing and material characterization. The *resonance method* is applied in this study with the purpose of demonstrating that this method is capable of non-destructively extracting a material's changes in structural properties. This method can also be used with sufficient precision on structures in operation for their condition monitoring.

# Chapter 2

# Theoretical analysis

## 2.1 Fracture behaviour of thin materials

The investigation of the fracture behaviour of thin materials is pervasive in the fracture mechanics community. Some important previous works related to paperboard can be found in [19, 20]. A thin aluminium of thickness $6.25\mu m$ was investigated in [21]. The fracture toughness measurement of such a thin foil is not covered by the ASTM standard [22] and therefore should be done for the material under investigation. For a specimen configuration shown in Figure 2.1, a Strip Yield Model (SYM) with an appropriate geometry correction factor

$$\sigma_c = \frac{2\sigma_b}{\pi} \arccos\left[\exp(-\frac{\pi K_c^2}{8a_0\phi^2\sigma_b^2})\right] \tag{2.1}$$

was found by Kao-Walter et al. [21] to correlate well with the experimental results. In equation (2.1), $\sigma_c$ is the stress at crack growth and $\sigma_b$ is the stress at break of the specimen with no crack. $K_c$ is the fracture toughness obtained from the experiments by increasing the crack length step by step, and $\phi$ is the geometry correction factor, found in [23]. The suitability of this modified SYM was later confirmed [24] for other single layers, Low Density PolyEthylene (LDPE) and paperboard, used in liquid packaging industries.

The idea of investigating several crack lengths step by step led to the motivation of implementing a more accurate method of monitoring the defect

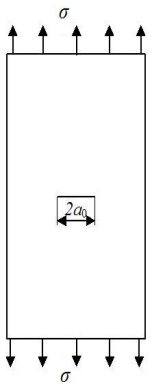


Figure 2.1: Centred crack panel specimen of size $230mm$ x $95mm$, with a crack length $2a_0$ varying from $5mm$ to $50mm$, under a remote stress $\sigma$

severity (crack propagation), or in general an inhomogeneity increase in the material. A remote acoustic method was chosen and initial work was done (paper A), showing a change in the spectrum response of the material to a harmonic excitation.

## 2.2 Vibration analysis

### 2.2.1 Governing equations

The theoretical analysis in this study uses the theory of vibrating membrane with account of intrinsic elasticity, governed by the equation [25]:

$$\frac{\partial^2 \xi}{\partial t^2} - c^2 \left( \frac{\partial^2 \xi}{\partial x^2} + \frac{\partial^2 \xi}{\partial y^2} \right) + d^2 \left( \frac{\partial^2 \xi}{\partial x^2} + \frac{\partial^2 \xi}{\partial y^2} \right)^2 = \frac{p\,(x, y, t)}{\rho h} \tag{2.2}$$

Here $\xi$- is the displacement normal to the plane *(xy)* coincident with the equilibrium position of membrane, $c$ - is the velocity of propagation of bending waves at zero intrinsic elasticity defined below, $p$ - is external pressure on the surface of the membrane, $\rho, h$ - are density and thickness of the material, and:

$$c = \sqrt{T/(\rho h)}, \quad d^2 = \frac{Eh^2}{12\rho\,(1-\nu^2)} \tag{2.3}$$

where $E$, $T$ and $\nu$ are the elastic modulus, tensile force per unit length of the edge, and the poisson's ratio.

The frequency equation with fixed-fixed boundary conditions (Figure 2.2(i)) was derived to obtain the vibration frequency of each bending mode as follows:

$$\omega_{mn} = c\sqrt{\left(\frac{\pi m}{a}\right)^2 + \left(\frac{\pi n}{b}\right)^2}\left\{1 + \frac{d^2}{2c^2}\left[\left(\frac{\pi m}{a}\right)^2 + \left(\frac{\pi n}{b}\right)^2\right]\right\}, \quad m = 0, 1, 2, 3, ... \tag{2.4}$$

$a$,$b$ are the dimensions of the membrane, $m$,$n$ are the mode numbers.

From the preceding equation, the frequency may shift because of material elasticity degradation (caused, for example, by accumulation of fatigue micro defects) as well as result of crack formation or local variation of density and thickness of the sheet.

### 2.2.2 Local density variation: addition of mass

Let the mass $m'$ be attached to the sheet as shown in Figure 2.2, and assume its size to be small in comparison with the wavelength of bending wave.

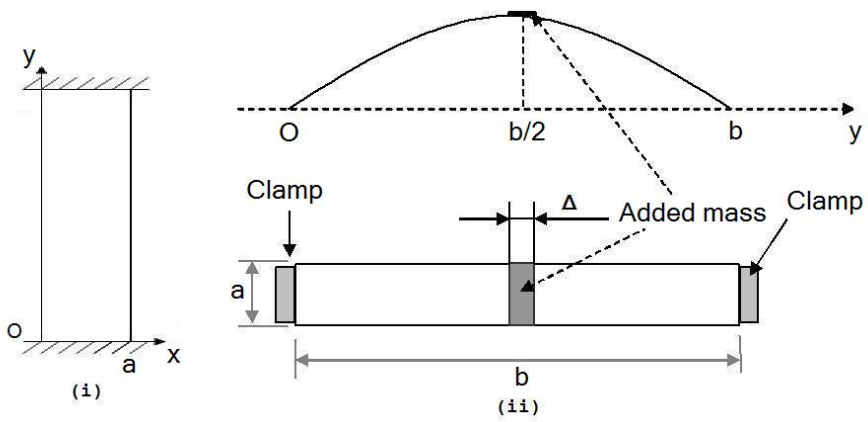


Figure 2.2: Specimen without (i) and with (ii) defect in form of added mass $m'$

This mass vibrates together with the membrane and yields the following

equation of natural frequencies:

$$\omega_{mn} = \Omega_{mn} \sqrt{\frac{1 + \frac{d^2}{c^4}\Omega_{mn}^2}{1 + 2\beta_q \frac{m'}{M} cos^2\left(\pi m \frac{x_0}{a}\right) sin^2\left(\pi n \frac{y_0}{b}\right)}}, \tag{2.5}$$

where $M = \rho hab$ - is the mass of the membrane, $\beta_0 = 1, \beta_q = 2\,(q > 1)$, and $\Omega_{mn}$ is the natural frequency of the unloaded membrane.

One can see that the local load shifts down the natural frequency. The shift is determined by the ratio of loading mass and the mass of membrane $\frac{m'}{M}$ . This shift can be detected only if the special mode is excited which has the loop neighboring the point $x_0, y_0$ of the location of the loading mass. Evidently, the weight placed in the node cannot shift the frequency of the corresponding mode.

This theory offers an idea of how one can detect inhomogeneity in form of added mass using a measurement of the frequency shift. Further details are included in paper B.

### 2.2.3 Presence of a crack

Let us consider a local opening without reduction of the global mass in the material as shown in Figure 2.3. For simplicity, the structure is assumed to be made of two sections of equal size, one of which contains the defect. Each of the sections I and II can be treated separately based on the theory presented above. Hence, sections I and II will vibrate at fundamental frequencies $\omega_1$ and $\omega_2$ respectively. If the two sections are joined to form one membrane, this membrane will vibrate at a frequency $\omega$, which lies between $\omega_1$ and $\omega_2$.

The frequency $\omega$ was derived in paper B and found to be expressed as follows:

$$\omega^2 = 2\frac{\pi^2}{b^2}\frac{c_1^2 c_2^2}{c_1^2 + c_2^2} \tag{2.6}$$

where $c_1$ and $c_2$ are the velocities of bending wave in sections I and II respectively.

Assuming $c_1^2 \approx c_2^2$ with $c_1 \equiv c$ and $c_2 \equiv c\,(1 - \delta)$, $\delta << 1$, we obtain the

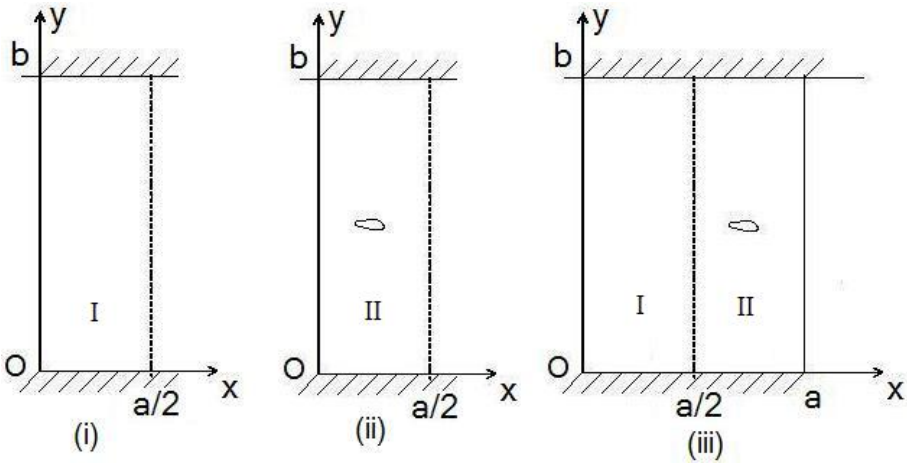


Figure 2.3: A hand-made crack

following relative frequency shift:

$$\omega = \omega_1 \left(1 - \frac{c_1 - c_2}{2c_1}\right) \tag{2.7}$$

If no crack exists, $c_2 = c_1$ and evidently $\omega = \omega_1$. As a crack is introduced, $c_2$ decreases slightly and the relative frequency shift increases. To use equation (2.4), another variable has to be known - the wave velocity or the depth of the discontinuity in the material (crack size in this case, or amount of added mass in the previous case). If the latter is not known, and this could be the reason for a subsequent investigation, the wave velocity has to be determined. Knowing the dimensions of the specimen, the method can then be used for velocity measurement.

Consequently, this theory offers an idea of how one can monitor a defect severity using the measurement of the frequency shift. Further details and results are found in paper C.

### 2.2.4 Young's modulus extraction from dynamic measurement

From equation (2.3) relating the velocity of bending wave and the tensile load $T$, one can easily derive the following:

$$c = \sqrt{T/(\rho h)} = \sqrt{\frac{E\epsilon}{\rho}} \tag{2.8}$$

where $\epsilon$ is the longitudinal strain.

Inserting equation (2.8) into equation (2.4) with no account of intrinsic elasticity, and solving for normal modes along the length of the specimen yield:

$$f_{on}^2 = \frac{E \cdot n^2}{4 \cdot \rho} \cdot \epsilon \tag{2.9}$$

where $f_{on}$ is the resonance frequency of mode $on$ in $Hz$. $E$, $n$ and $\rho$ being all constants for a given measurement, the square resonance frequency is linearly proportional to the strain. As a consequence, the dynamic Young's modulus is extracted from the slope of the curve.

Equation (2.9) offers an idea of how one can estimate the Young's modulus of a material from a dynamic measurement using as inputs the longitudinal strain and the measurement of the corresponding resonance frequency in flexural mode. This approach also emphasizes the feasibility of health monitoring through a change in time of the dynamic Young's modulus due to a possible occurrence of residual strain within the investigated material. Further details and results are presented in paper D.

# Chapter 3

# Method and Measurement Parameters

## 3.1 Specimen configuration

The material under investigation is flat rectangular shaped, so that the elastic characterization can easily be performed by stretching or vibrating tests applied to a clamped specimen as shown in Figure 3.1. This kind of specimen in static or dynamic mechanical tests allows the achievement of more repeatable results as illustrated for polycrystalline plates in references [26–30].

A specimen with an inhomogeneity in form of local density variation is as shown in Figure 2.2(ii), while a specimen with a crack is illustrated in Figure 2.3(ii).

## 3.2 The static approach

This approach uses the tensile test, also known as tension test. It is probably the most fundamental type of mechanical test one can perform on materials. Tensile tests are fully standardized, though not yet for all materials as thin as our material of interest.

The material is pulled until it breaks, and a complete tensile profile is obtained. A curve then results, showing how the material reacts to the forces

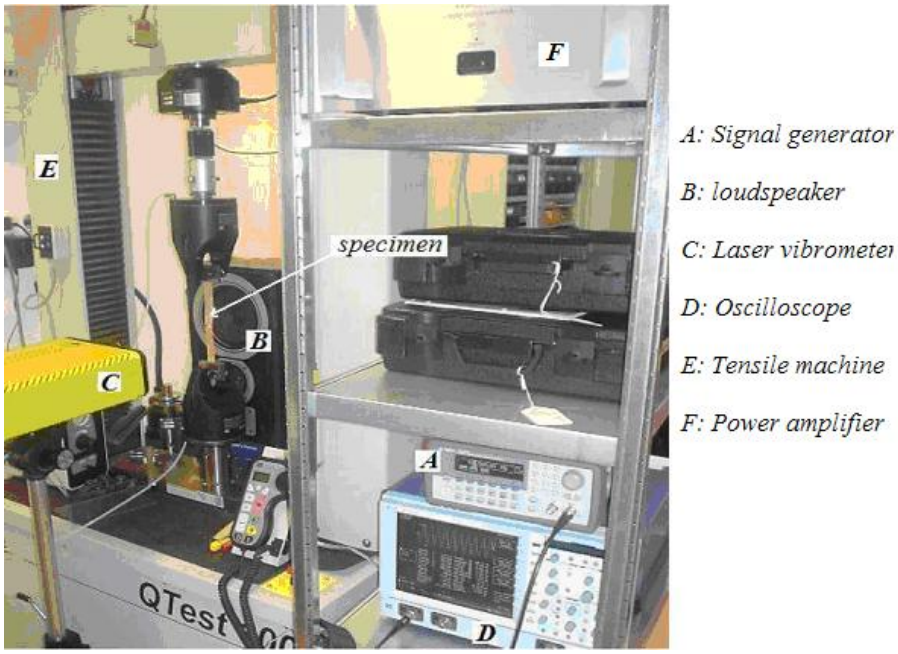


Figure 3.1: Testing equipment

being applied. For most tensile testing of materials, the relationship between the applied force, or load, and the elongation of the specimen in the initial portion of the test is linear. In this linear region, the line obeys the relationship defined as 'Hooke's law' where the ratio of stress to strain is a constant, or $\frac{\sigma}{\epsilon} = E$ . $E$ is the slope of the line in this region where stress $\sigma$ is proportional to strain $\epsilon$ and is called the *modulus of elasticity* or *Young's modulus*.

This approach was used for the estimation of the fracture toughness of non standard specimens; a detailed procedure can be found in [24].

## 3.3 The dynamic approach

### 3.3.1 Methodology

This approach is based on the relation between the mechanical resonance frequencies and the dynamic elastic constants of the material; this correlation depends on the geometry and on the mass of the specimen. The standard [31] suggests using bar-, rod- or circular plate-shaped specimens: it requires the

measurement of the natural frequency in two different modes of vibration and provides the procedures for determining the elastic constants. Flat plates of non circular shape can also be used, but the equations for determining the elastic constants are not provided by the standards and must be evaluated separately, motivating the implementation of the new method presented in this study.

For this purpose, a simple set-up for remote testing is suggested as illustrated in Figure 3.2. The sheet material is placed between two grips of a testing machine performing the tensile test. The static loading gives elastic properties to the thin sheet, and transverse vibrations can be excited. The intrinsic elasticity of some materials has to be taken into consideration. Vibrations are excited using a non-contact acoustic technique, and resonance is detected using a laser vibrometer. The resonant frequency of the thin sheet can then be utilized in a model for damage assessment or to extract the Young's modulus of elasticity. Instead of tensile machine, rotating cylinders setting the conveyer belt in motion are used sometimes for straining.

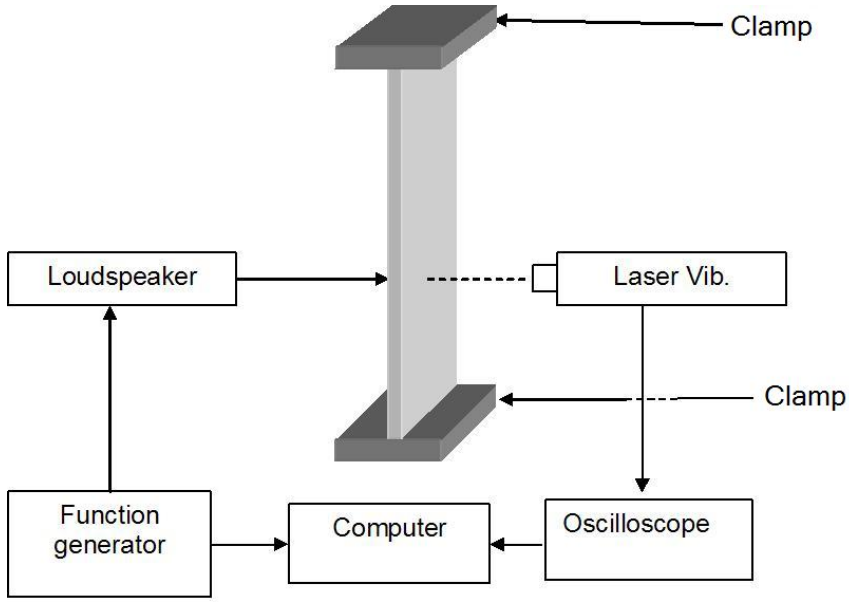


Figure 3.2: Bloc diagram of the acoustic measurement experimental setup

The actual measured variable is the resonance frequency, obtained as described below.

### 3.3.2 Resonance frequency and material characterization

For excitation of the tested structures, a loudspeaker is placed at the backside of the specimen (see Figure 3.1 or Figure 3.2). A function generator is used to create a sinusoidal signal that first passes through an amplifier (if required) and then is sent to the loudspeaker. A wave is then produced by the sound pressure from the remote loudspeaker, exciting transverse vibrations on the material.

The displacement of a single point on the test specimen is detected using a Laser Doppler Vibrometer (LDV). The displacement or velocity signal is sent from the LDV controller to an oscilloscope. The resonant frequency of the structure is determined by sweeping through frequencies with the function generator, observing the amplitude of the waveform on the oscilloscope, and recording the frequency at which the peak occurs. Using this method the resonant frequency of each sample is found.

At a given constant strain, the resonance frequency is experimentally monitored for an increasing inhomogeneity in form of added mass (see equation (2.5)) and in form of crack (see equation (2.7)) for damage severity assessment.

For a varying strain (or extension) within elastic region of the material, equation (2.9) is plotted using experimental data for each sample. A set of measured data is shown in Table 3.1. A basic fitting is performed using a linear

| Extension $[mm]$ | 0.5 | 0.6 | 0.7 | 0.8 |
|---|---|---|---|---|
| Res. freq. mode 1 $[Hz]$ | 335 | 414 | 474 | 523 |
| Res. freq. mode 2 $[Hz]$ | 590 | 861 | 943 | 1032 |
| Res. freq. mode 3 $[Hz]$ | 887 | 1055 | 1177 | 1300 |
| Res. freq. mode 4 $[Hz]$ | 1442 | 1638 | 1775 | 2050 |

Table 3.1: A set of measured data in dynamic measurement on paperboard of size $150mm$ x $15mm$

interpolation method, and a linear function is obtained as shown in Figure 3.3 for the fundamental mode on paperboard. The slope of the line obtained,

according to equation (2.9), allows the extraction of the Youngs modulus.

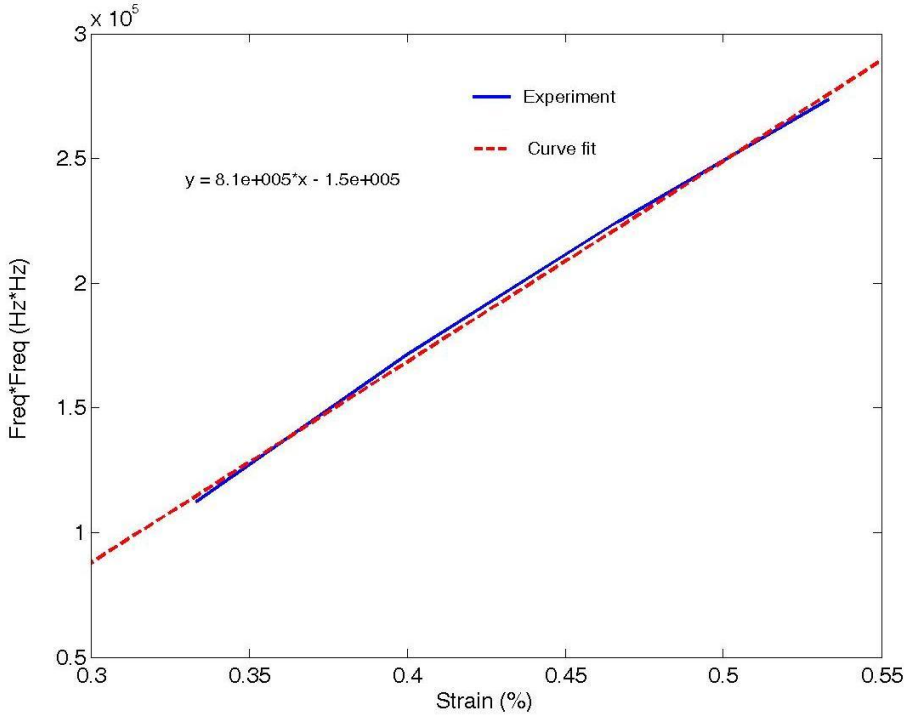


Figure 3.3: A typical $f^2$ vs. $\epsilon$ plot for extraction of Young's modulus (obtained from testing of paperboard)

# Chapter 4

# Results and discussions

The fracture behaviour was investigated on specimens of length $230mm$ and width $95mm$. The crack length was increased step by step from $5mm$ to $50mm$. Figure 4.1, Figure 4.2, and Figure 4.3 show good agreement of the modified SYM by Kao-Walter et al. ([21]) with the experiment.

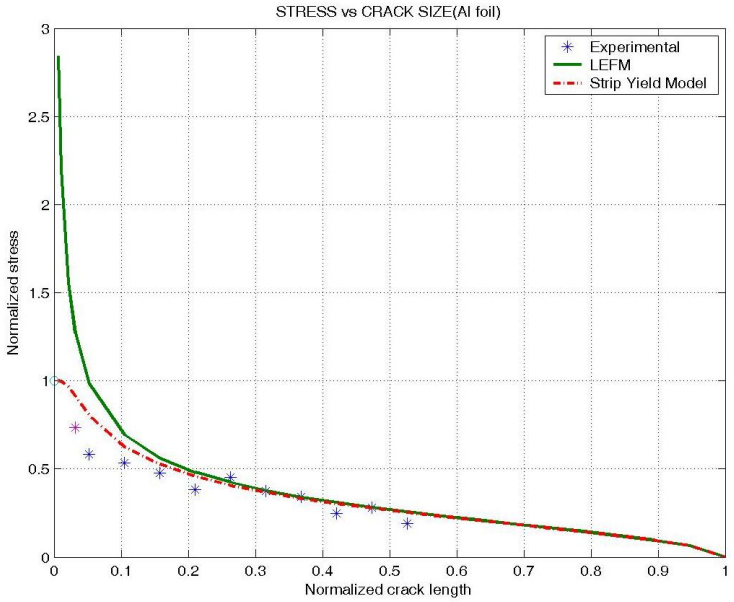


Figure 4.1: Normalized stress vs crack length: Aluminium foil

For the purpose of estimating a material's fracture property such as

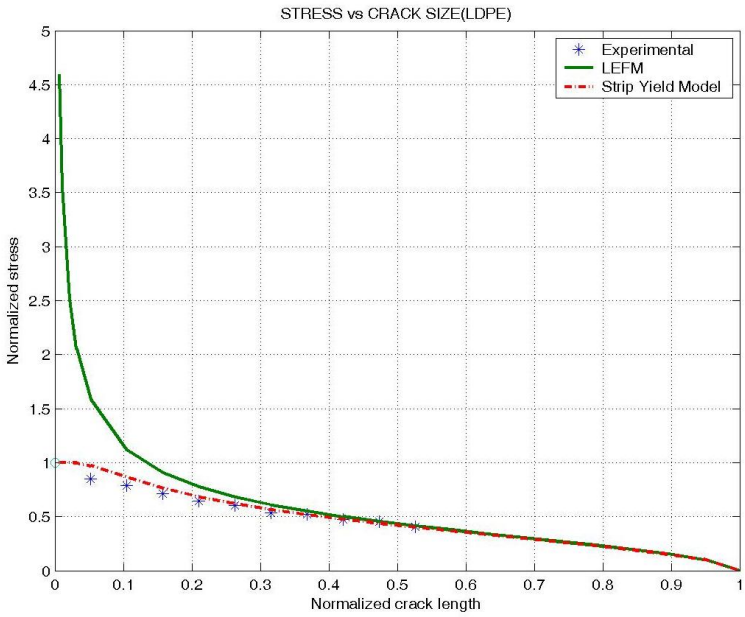


Figure 4.2: Normalized stress vs crack length: LDPE

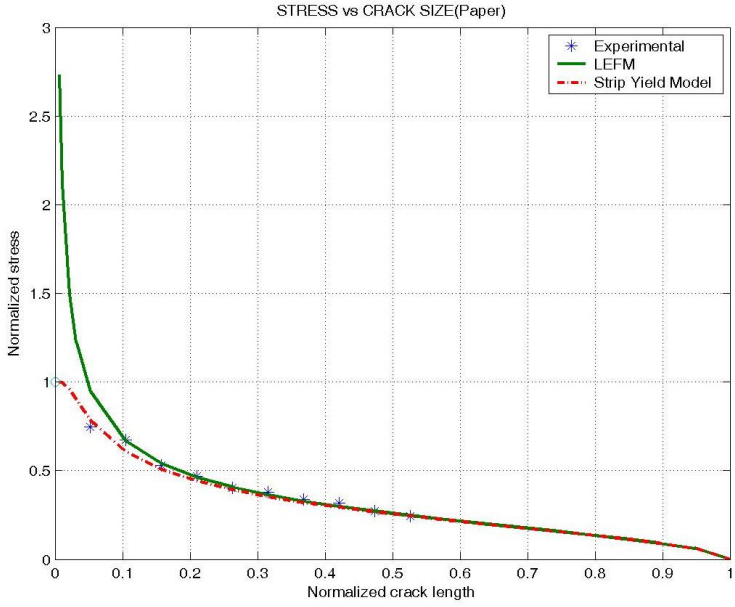


Figure 4.3: Normalized stress vs crack length: Paperboard

the fracture toughness, a real-time monitoring of the crack propagation is needed. Figure 4.4 shows the feasibility of a nondestructive method for such a monitoring process. The resonance frequency of the vibrating specimen is shifted as the crack length increases.

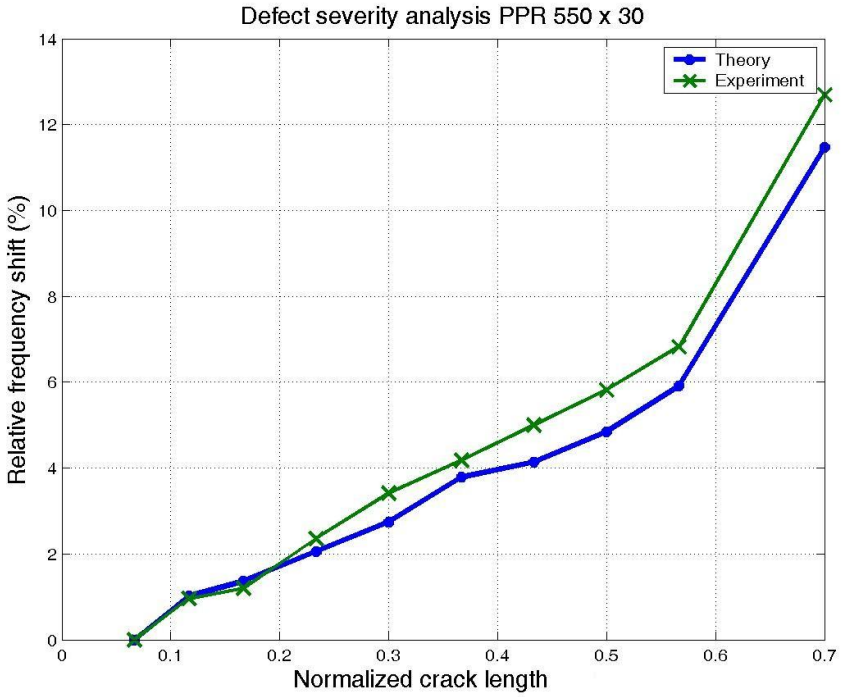


Figure 4.4: Frequency shift vs crack length: Paperboard of length $550mm$ and width $95mm$

The detection of a inhomogeneity in form of mass addition is also a result of this work, as illustrated in Figure 4.5. The specimen was a paperboard of size 650mm x 12mm x 0.1mm, preloaded at 17N in order to make it a structural element. Small strips (2.25% of the total mass of the specimen) were successively added to the middle of the specimen and the fundamental frequency shift was monitored.

Figure 4.6 shows the estimation of the Young's modulus of LDPE and paperboard using static and dynamic measurements. The Young's modulus

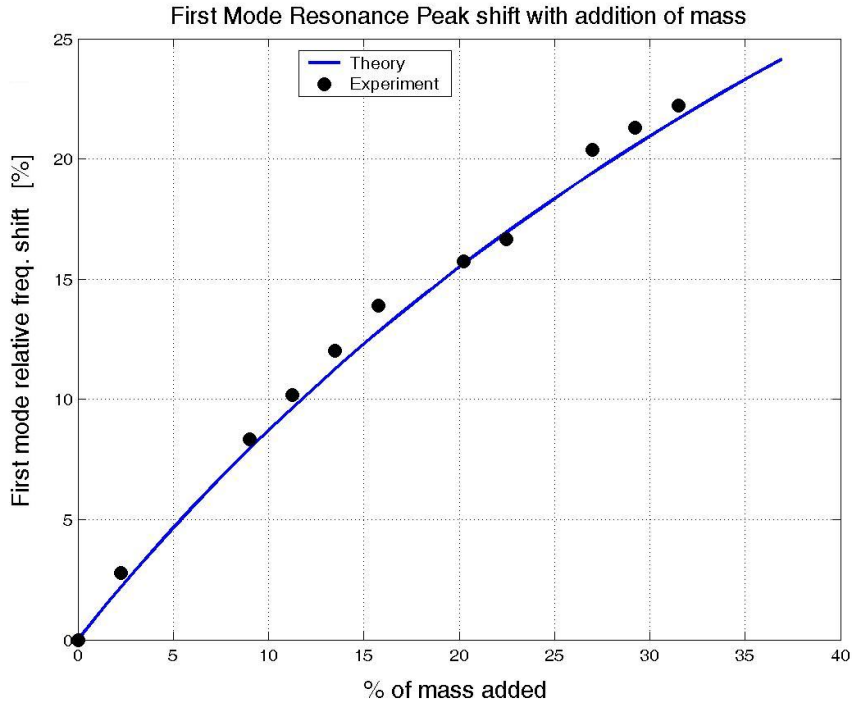


Figure 4.5: First mode relative frequency shift with addition of mass, from equation (2.5)

from the dynamic measurement is lower. A possible reason is that the modes are not pure bending along the length of the specimen, which is not taken into consideration in the derivation of equations. Although this is a limitation, the result allows to consider the suggested method as an alternative for the purpose of structural health monitoring of materials of specific sizes. The stiffness of the material changes with introduction of a defect, which can be monitored at a certain interval of time. Therefore, the Youngs modulus being estimated from natural frequencies, the method confirms the use of the latter for defect detection. This issue was previously mentionned by Van'kov et al.[32].

However, the modal frequency is a global property of the structure; therefore a shift in this parameter may not be used to identify more than the presence of damage. In other words, the frequency generally cannot provide

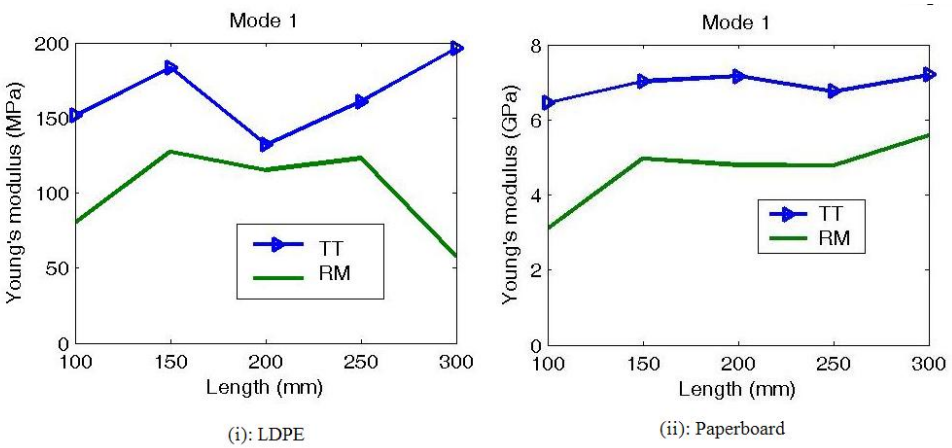


Figure 4.6: Young's modulus from static and dynamic methods: TT=Tensile Test (static), RM=Resonance Method (dynamic)

spatial information about structural changes. Meanwhile, there is an exception to this limitation at higher modal frequencies, where the modes are associated with local responses. Therefore, the practical limitations involved with the excitation and extraction of these local modes, caused in part by high modal density, can make them difficult to identify.

# Chapter 5

# Summary of papers

## 5.1 Paper A

This paper considers the study of the fracture behavior of paperboard (thickness 100$\mu$m). The measurement of the plane stress fracture toughness is performed and a modified SYM is shown to be suitable for the study of the fracture behavior of this material. Estimation of the fracture toughness, defined as the strength of the material in presence of a crack, is performed at several increasing crack lengths simulating crack propagation. This approach can be considered a health monitoring technique, leading to the motivation of introducing a NDT method for the investigation of the material. The low frequency vibration-based technique is then employed and yields the detection of the presence of a crack in the material, through a remote excitation and sensing method.

## 5.2 Paper B

Considering the possibility of low frequency range detection of the presence of defect observed in paper A for thin sheets, this paper considers the development of a new theory illustrating the feasibility of the detection of inhomogeneity in forms of crack and added mass on sheet materials, using the measurement of the frequency shift. The agreement between theoretical and

experimental results is good, making the low frequency vibration-based a potential method for non-destructive testing of sheet materials.

## 5.3 Paper C

In this paper, a new modality for nondestructive testing and characterization of sheet materials is considered. The vibration-based technique suggested in paper A and B is shown to be capable of monitoring an increase in defect severity. The work also emphasizes the feasibility of mechanical characterization of sheet materials with no intrinsic elasticity (not covered by existing standard methods) by the measurement of the strain dependent resonance frequency in flexural mode.

## 5.4 Paper D

Preliminary indications of the use of low frequency vibration-based for material characterization were given in paper C. This paper extensively focuses on that issue by showing both theoretically and experimentally that bending resonance can be utilized to nondestructively extract the Young's modulus of thin sheets. It follows that the method is capable of monitoring the change in material properties in time for the purpose of in-service diagnosis of structures and failure prevention.

# Chapter 6

# Conclusions and Further Work

This thesis addresses a structural health monitoring strategy based on dynamic structural analysis of sheet materials at low frequency range, which is new in the engineering community. It also concerns the monitoring of the resonance frequency for the purpose of material characterization. The frequency band of investigation spans from 0 up to a maximum of 2 kHz, thus allowing the use of an ordinary and inexpensive loudspeaker for remote excitation. A Laser Doppler Vibrometer is used for sensing selected single points. The main result of this thesis is the proof, both theoretical and experimental, that low frequency acoustics can be used for non-destructive testing and characterization of sheet materials. Although liable to improvement, this groundwork is accurate enough for acoustic weighing, capable of monitoring changes in modal properties and thus, capable of assessing defect severity. The observation that changes in structural properties cause changes in vibration frequencies is the impetus for using modal methods for health monitoring and material characterization.

Various other applications can be predicted such as a rigorous detection of residual stress and strain, fatigue damage, and more. Therefore, it shows the feasibility of the presented new technique to in-service thin sheets characterization for the purpose of condition monitoring. Indeed, the residual

stress, responsible for stress-related failure of component in-service, is usually measured indirectly by measuring the residual strain of the structure and multiplying it by a value for elastic modulus. However, elastic modulus for thin sheets can vary from process to process, and this work provides an easily executed method for determining the local elastic modulus needed to accurately determine the stress in the structure.

Meanwhile, modal parameters are normally less sensitive to localized defects, but generally provide indications regarding global changes as a result of damage and potentially estimate their severity. In parallel to modal monitoring at higher modes of investigation, the Scanning Laser Doppler Vibrometer may be used, which measures the velocity of the structure at points on a user-defined grid, thus providing an unprecedented amount of information on a possible defect.

Future research in the field of vibration-based condition monitoring and material characterization then appears unavoidable. There is a significant need in this field for research on the integration of theoretical algorithms with application-specific knowledge bases and practical experimental constraints. Overall, it is obvious that sufficient evidence exists to promote the use of measured vibration data for the monitoring of damage evolution in structures as well as materials elastic property characterization, using harmonic remote excitation signals. It is clear, though, that the literature in general needs to be more focused on the specific applications and industries that would benefit from this technology, such as health monitoring of structures with long design life, life-safety implications and high capital expenditures.

Additionally, research should be focused more on testing of real structures in their operating environment, rather than laboratory tests of representative structures. Because of the magnitude of such projects, more cooperation will be required between academia, industry, and government organizations. If specific techniques can be developed to quantify and extend the life of structures, the investment made in this technology will clearly be worthwhile.

# Bibliography


[1] Doherty J. E. *Nondestructive Evaluation: Handbook on Experimental Mechanics*. Society for Experimental Mechanics, Inc., a. s. kobayashi edition, 1987.

[2] Zheng Y., Maev R., and Solodov I.Y. Nonlinear acoustic applications for material characterization: a review. *Canadian Journal of Physics*, **77**:1–41, 1999.

[3] Hedberg C. M. and Rudenko O. V. Pulse response of a nonlinear layer. *Acoustical Society of America*, **110** (5):Pt.1, 2000.

[4] Rudenko O. V., Sobisevich L. E., Sobisevich A. L., and Hedberg C. M. Nonlinear response of a layer to pulse action in diagnostics of small inhomogeneities. *Doklady Physics*, **45** (9):485–488, 2000.

[5] Doebling S. W., Farrar C. R., Prime M. B., and Shevitz D. W. Damage identification and health monitoring of structural and mechanical systems from changes in their vibration characteristics: a literature review. *Los Alamos National Laboratory report LA-13070-MS*, April 1996.

[6] Rytter A. Vibration based inspection of civil engineering structures. *Department of Building Technology and Structural Engineering, AalborgUniversity, Denmark*, Ph. D. Dissertation, 1993.

[7] Vandiver J.K. Detection of structural failure onfixed platforms by measurement of dynamic response. *Journal of Petroleum Technology*, pages 305–310, 1977.

[8] Begg R. D., Mackenzie A. C.and Dodds C. J., and O. Loland. Structural integrity monitoring using digital processing of vibration signals. *in Proc. 8th Annual Offshore Tech. Conf.*, pages 305–311, 1976.

[9] Whittome T.R. and C.J. Dodds. Monitoring offshore structures by vibration techniques. *in Proc. of Design in Offshore Structures Conference*, pages 93–100, 1983.

[10] Cawley P. and R. D. Adams. The locations of defects in structures from measurements of natural frequencies. *Journal of Strain Analysis*, **14** (2):49–57, 1979.

[11] Friswell M. I., Penny J. E. T., and Wilson D. A. L. Using vibration data and statistical measures to locate damage in structures. *The International Journal of Analytical and Experimental Modal Analysis*, **9**(4):239–254, 1994.

[12] Gudmundson P. Eigenfrequency changes of structures due to cracks, notches, or other geometrical changes. *Journal of the Mechanics and Physics of Solids*, **30**(5):339–353, 1982.

[13] Dalgleish B. J., Fakhr A., Pratt P. L., and Rawlings R. D. The temperature dependence of the fracture toughness and acoustic emission of polycrystalline alumina. *Journal of Materials Science*, **14**, No.11:2605–2615, 1979.

[15] Hashida T. Fracture toughness testing of core-based specimens by acoustic emission. *International journal of rock mechanics and mining sciences geomechanics abstracts*, **30**, No.1:61–69, 1993.

[14] Nasseri M. H. B., Mohanty B., and Young R. P. Fracture toughness measurements and acoustic emission activity in brittle rocks. *Pure and Applied Geophysics*, **163**, Issue 5-6:917–945, 2006.

[16] Naugolnykh K.A. and Ostrovsky L.A. Nonlinear wave process in acoustics. *Cambridge University Press, Cambridge*, 1998.

[17] Kao-Walter S. On the fracture of thin laminates. *Doctoral Dissertation*, ISSN 1650-2159, ISBN 91-7295-048-X, 2004.

[18] Smee S. A., Gaitan M., Novotny D. B., Joshi Y., and Blackburn D. L. Ic test structures for multi-layer stress determination. *IEEE Electron Device Letters*, **21**, No.1:12–14, 2000.

[19] Tryding J. In-plane fracture of paper. *Ph.D thesis, Report TVSM-1008, ISSN: 0281-6679*, Lund University, Sweden, 1996.

[20] Xia Q. S. Mechanics of inelastic deformation and delamination in paperboard. *Ph.D thesis, Dept. of Mech. Eng.*, Massachusetts Institute of Technology, USA:Pt.1, 2002.

[21] Kao-Walter S. and Ståhle P. Fracture behaviour of a thin al-foil - measuring and modelling of the fracture processes. *SPIE 3rd ICEM proceedings*, ISBN: 0-8194-4261-5:253–256, Beijing, China, 2001.

[22] ASTM D-882-91. Standard test method for tensile properties of thin plastic sheeting. *American Society for Testing and Materials*, Philadelphia, Pa., 1991.

[23] Anderson T. L. *Fracture Mechanics: Fundamentals and Applications*. ISBN: 0-8493-4260-0, Florida, USA, crc press llc edition, 1995.

[24] Mfoumou E. M. and Kao-Walter S. Fracture toughness testing of non standard specimens. *Research report No 2004:05*, Blekinge Institute of Technology, Sweden, 2004.

[25] Landau L. D. and Lifshitz E. M. Theory of elasticity. *3r Edition, Pergamon*, 1979.

[26] Valentine T.J., Whitehead A. J., Sussmann R. S., Wort C. J., and Scarsbrook G. A. Mechanical property measurements of bulk pollycrystalline cvd diamond. *Diamond Related Materials*, **3**:1168–1172, 1994.

[27] Werner M., Klose S., Szucs, Molle C., Fecht H. J., and Johnson C. et al. High temperature young's modulus of pollycrystalline diamond. *Diamond Related Materials*, **6**:344–347, 1997.

[28] Szuecs F., Werner M., Sussmann R. S., Pickles C. S. J., and Fecht H. J. Temperature dependence of young's modulus and degradation of chemical vapor deposited diamond. *Journal of Applied Physics*, **86**(11):6010–6017, 1999.

[29] Develyn M. P. and Taniguchi T. Elastic properties of translucent polycrystalline cubic boron nitride as characterized by the dynamic resonance method. *Diamond Related Materials*, **8**:1522–1526, 1999.

[30] Werner M., Kohler T., Mietke S., Worner E., Johnson C., and Fecht H. J. Review on the non-destructive characterization and application of doped and undoped polycrystalline diamond films. *Proc. SPIE*, **4703**:199–210, 2002.

[31] ASTM E1876-00e1. Standard test method for dynamic young's modulus, shear modulus, and poisson's ratio by impulse excitation of vibration. *Annual Book of ASTM Standard*, **03**-01, 2001.

[32] Van'kov Yu. V., Kazakov R. B., and Yakovleva E. R. Natural frequencies as diagnostic criteria for flaw detection. *Electronic Journal Technical Acoustics, http://www.ejta.org*, 5, 2003.

# Appendix A

# Appended papers

# Paper A

# Fracture Mechanism and Acoustic Damage Analysis of Thin Materials

**Paper A is published as:**

Mfoumou, E., Kao-Walter, S., and Hedberg, C., "Fracture Mechanism and Acoustic Damage Analysis of Thin Materials", *pp 1248 in Proceedings of the 11th International Conference on Fracture, Turin, Italy (2005).*

# Fracture Mechanism and Acoustic Damage Analysis of Thin Materials

Mfoumou, E. M., Kao-Walter, S., and Hedberg, C.

**Abstract**

The fracture behavior of paper board ($100\mu m$) used in food packaging material is studied. The plane stress fracture toughness is measured based on a centered crack panel. Different crack sizes have been tested. A compromise (crack length) was found, at which Strip Yield Model as well as Linear Elastic Fracture Mechanics allow the validation of experimental results. Meanwhile, accurate results are obtained using the Strip Yield Model with a geometric correction.

Besides, detection of damage in food packaging material is an interesting feature in quality control of the product. Therefore the material is investigated using an acoustic method. The method consists of a vibration-based damage assessment and leads to a first level differentiation between damaged and non-damaged specimens.

## 1 Introduction

Most of the liquid food packaging materials use to consist of several different layers of material for the different requirements. Examples are aluminium foil (Al), Low Density Polyethylene (LDPE), and Carton (PPR). It is important to secure that every layer keeps its function during the forming, filling and transportation process. Mechanical properties of these materials have been studied [1, 2, 3, 4, 5]. The fracture behaviour of Al-foil (about 6-7$\mu m$) was investigated [6] and the fracture toughness was found to be much lower than what is given in standard materials handbooks. However, a fracture mechanical model of such thin materials was suggested.

The purpose and aim of this work is to extend the results from [6] through investigation of the fracture behaviour of paper board (thickness=$100\mu m$, and density=$0.684g/cm^3$). The specificity of this continuation study is still the non standard specimen size, particularly the thickness which does not satisfy the ASTM

standard No E399 [8]. The study uses experimental method and theoretical analysis to determine a reliable modelling method for approximating the thin material under consideration. Fracture toughness is characterized and measured using the method suggested in [7].

Attempt is also made to apply a nondestructive technique for differentiation between non-damaged and damaged specimens. Since fracture process in laminated packaging material could start on the inner layers, making it difficult to see, investigation is made using an acoustic method and modal parameters of the material. There exists an extensive literature on the subject of damage detection using modal parameters [9, 10, 11]. Emphasis is put here on the "level 1" vibration-based damage assessment established by Doebling et al. [11].

## 2 Theoretical Analysis

At onset of crack growth a relation between stress and stress intensity factor can be derived by LEFM [12]:

$$\sigma_c = \frac{K_c}{\sqrt{\pi \cdot a} \cdot \varphi\left(\frac{a}{w}\right)} \tag{1}$$

with

$$\varphi\left(\frac{a}{w}\right) = \sqrt{sec(\frac{\pi \cdot a}{2 \cdot w})} \cdot \left[1 - 0.025 \cdot \left(\frac{a}{w}\right)^2 + 0.06 \cdot \left(\frac{a}{w}\right)^4\right] \tag{2}$$

where $a$ is half the crack length, $w$ is half the width, $B$ is the thickness, $\sigma_c$ is the peak stress for the given initial crack length, and $K_c$ the fracture toughness obtained experimentally (based on the reasonable crack length for the purpose).

The Strip Yield Model with the appropriate geometry correction factor $\varphi$ , derived in [6], is expressed as follows

$$\sigma_c = \frac{2 \cdot \sigma_b}{\pi} \cdot asec\left[\exp(\frac{\pi \cdot K_c^2}{8 \cdot a \cdot \phi^2 \cdot \sigma_b^2})\right] \tag{3}$$

where $\sigma_b$ is the stress at break from tensile test, see [13] for details.

For damage detection through changes in basic modal properties, theory of forced oscillation of membrane (well known in physical acoustics) is used on a specimen configuration shown in fig:fig1, with the external pressure derived from Newton's second law of motion, as shown by the system of equations

$$\frac{\partial^2 \xi}{\partial t^2} - c^2 \cdot \frac{\partial^2 \xi}{\partial y^2} = \frac{p(y,t)}{\rho \cdot h}, \tag{4}$$

and

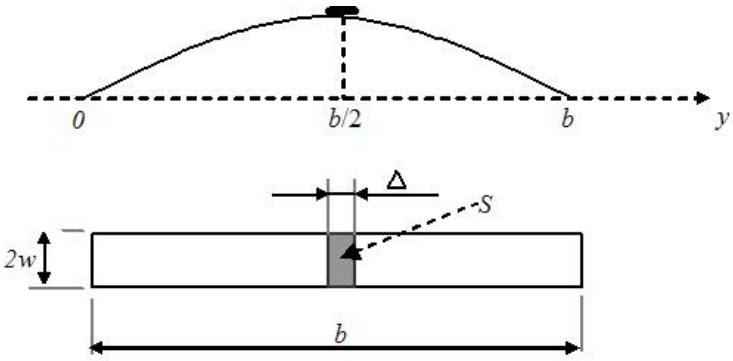


Figure 1: Specimen configuration

$$m \cdot \frac{d^2\xi\left(\frac{b}{2}\right)}{dt^2} = -p \cdot S = -p \cdot 2w \cdot \Delta \tag{5}$$

with

$$c = \sqrt{\frac{T}{\rho \cdot h}} \tag{6}$$

where $T$ is the load per unit length, $\rho$ the density and $h$ the thickness of the specimen, $m$ is the added mass, $p$ the external pressure which acts on the membrane, and $\xi$ the transversal displacement of membrane. The strip with area $S$ is roughly assumed to be either a positive mass (addition of mass), or a negative mass (hole or removal of matter).

The above system of equations reduces to the following:

$$\frac{\partial^2\xi}{\partial t^2} - c^2 \cdot \frac{\partial^2\xi}{\partial y^2} = \frac{m}{\rho \cdot h \cdot 2 \cdot w \cdot \Delta} \cdot \frac{d^2\xi\left(\frac{b}{2}\right)}{dt^2} = \left\{ \begin{matrix} 1,\ if\ (\frac{b}{2}-\frac{\Delta}{2}) < y < (\frac{b}{2}+\frac{\Delta}{2}) \\ 0, \quad otherwise \end{matrix} \right\} \tag{7}$$

For a harmonic excitation and looking for low frequency modes, we write:

$$\xi = A \cdot cos(w \cdot t) \cdot sin(\frac{\pi}{b}y) \tag{8}$$

Introducing equation (8) into equation (7), multiplying each side of the equation by $sin(\frac{\pi}{b}y)$, and integrating over 0 and $b$ lead to the following,

$$\frac{w}{w_0} = \frac{1}{\sqrt{1+2\frac{m}{M}}} \approx 1 - \frac{m}{M} \quad \Longrightarrow \quad f \approx f_0 \cdot (1 + 2\frac{m}{M}) \tag{9}$$

where $f_0$ is the fundamental frequency without adding a mass on the specimen, $f$ the new first mode, and $M$ the mass of the membrane.

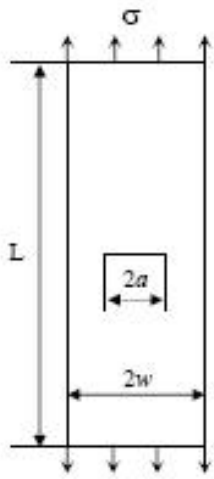


Figure 2: Centred crack panel

## 3 Experimental method

Center cracked panels as shown in figure 2 are investigated. The MTS Tensile Test Machine is used. The load on the sample is recorded by a piezo-electric load cell mounted between the sample and the crosshead. A 2.5 $kN$ loadcell is used, with a pair of wide clamps see figure 3. The grip separation is set to the specimen length.

Experiment 1 is related to the evaluation of the strength of the material in presence of damage. A "hand-made" notch is performed using a razor blade, with length ranging from $2a = 5$ $mm$ to $2a = 50$ $mm$. The width and gauge length of the specimen are $2w = 95$ $mm$ and $L = 230$ $mm$ respectively. The test speed is 9.2 $mm/min$, and tests are run until the entire cross section breaks.

Experiment 2 is related to vibration-based damage assessment. Specimens without and with damage are considered. For the later, the "hand-made" notch performed has the length $2a = 6$ $mm$. The width and gauge length of the specimen are $2w = 12$ $mm$ and $L = 650$ $mm$ respectively. The test speed is 2 $mm/min$, and the crosshead is stopped when the load reaches 21 $N$. A low frequency loudspeaker is used to excite bending waves on the clamped specimen, and sensing is performed with a laser beam. The excitation signal is generated by an Agilent 33250 waveform generator, and the response is analyzed in a LeCroy Waverunner LT 364.

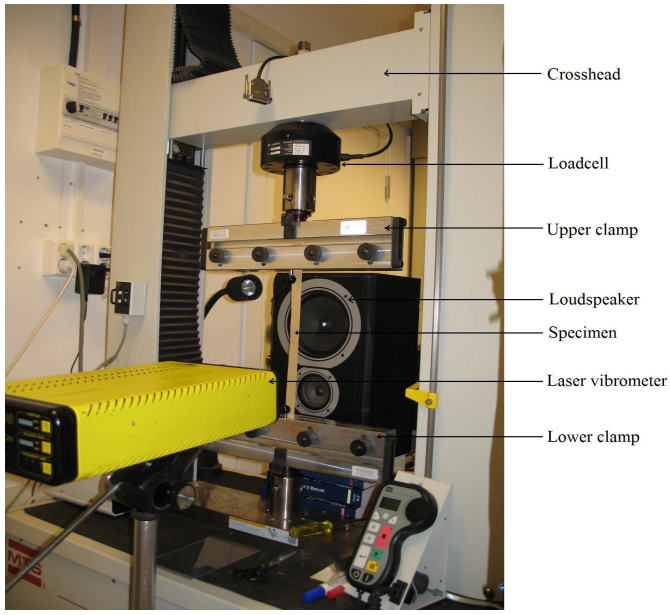


Figure 3: Setup for vibration-based investigation

# 4 Results and discussion

Critical stresses for different crack length (up to 50 $mm$) were measured by experiment. Normalized critical stress versus crack length curves for experiment, LEFM equation (1) and SYM equation (3) are plotted in figure 4. Good agreement is found between the measured results and the analytical results both with LEFM and SYM for crack lengths larger than $2a = 20$ $mm$. Meanwhile, for crack lengths less than 20 $mm$, SYM shows a better correlation with the measured values, whereas LEFM fails to describe the experimental result for such short crack lengths. A compromise is found at $2a = 45$ $mm$, and leads to $K_c = 3.12$ $MPa.m^{1/2}$.

Figure 5 shows a difference between damaged and undamaged specimens in experiment 2. Only odd harmonics are generated because of the position of laser beam. A new spectral line appears above the first mode, indicating presence of damage; this leads to a mode shift to the right of the fundamental.

Figure 6 shows the influence of adding mass on the first mode; this leads to mode shift to the left.

The current results confirm Doeblin et al. [11] speculation on damage detection by changes in the dynamic properties or response of systems in a qualitative manner, using acoustic techniques. However, the basic idea remains that commonly measured modal parameters (specifically frequencies, mode shapes, and modal damping) are functions of the physical properties of the structure (mass,

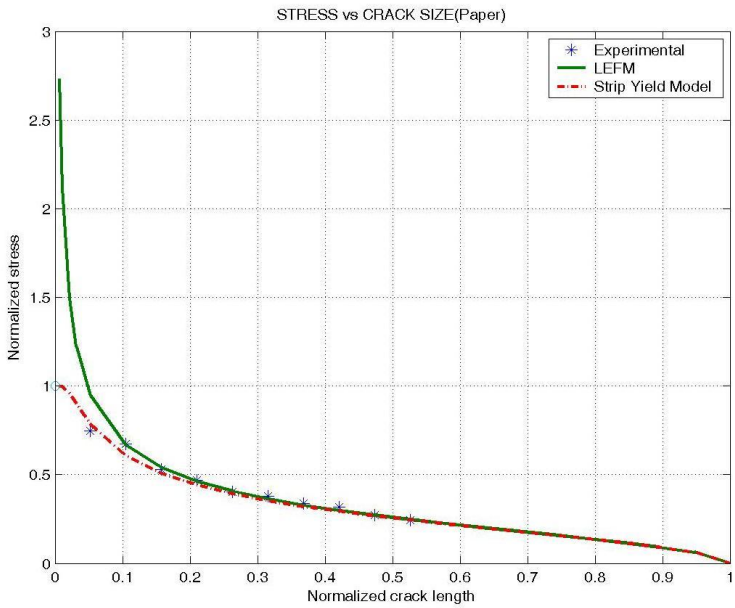


Figure 4: Normalized stress vs. crack length

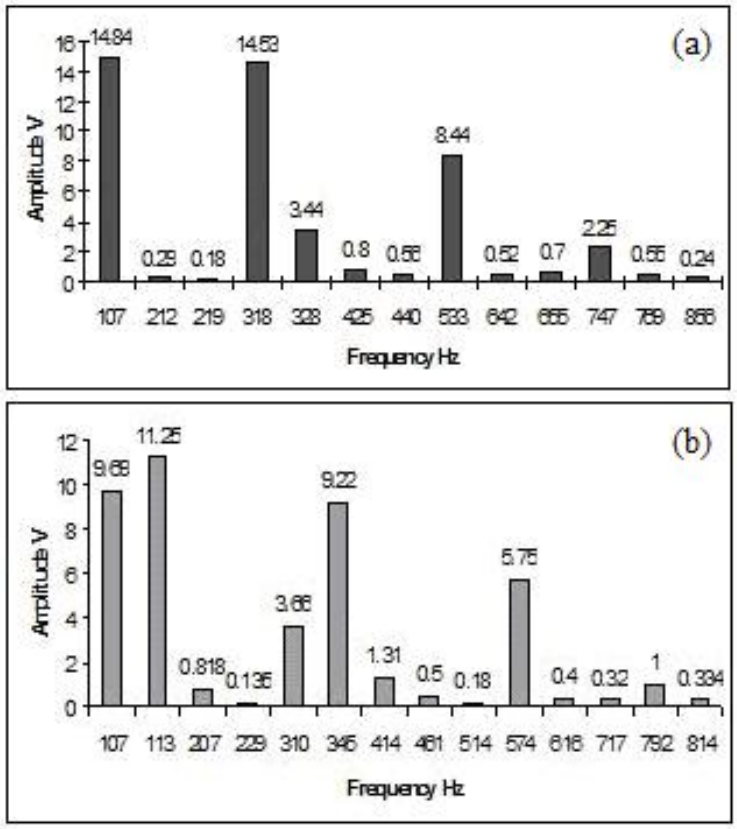


Figure 5: Dynamic response of the specimen: (a) undamaged, (b) damaged

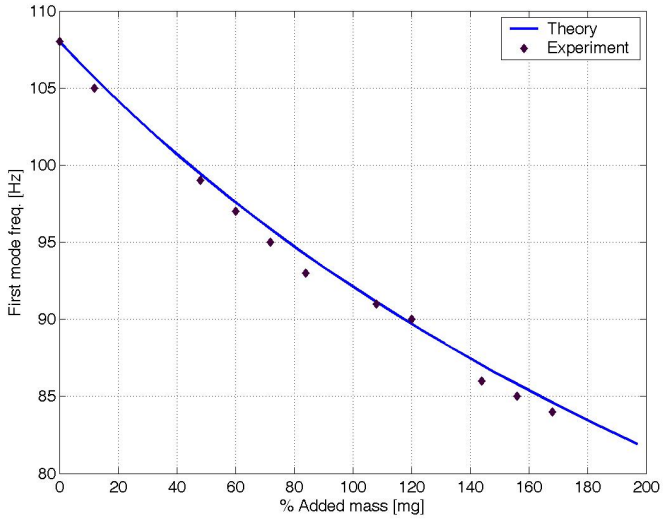


Figure 6: Fundamental mode frequency shift to higher range with added mass

damping, and stiffness). Consequently, changes in the physical properties, such as reductions in stiffness resulting from the onset of cracks or loosening of a connection, will cause detectable changes in these modal properties.

# 5 Conclusion

An experimental investigation was performed for the determination of plane stress fracture toughness for non standard materials. A single layer (paper board) from a laminated liquid food packaging material was tested. The result can be concluded as follows:

- The modified strip yield model developed in [6] was found to suit the material under investigation.

- As found in [6] for aluminium foil, a compromise was found at crack length $2a = 45\ mm$, at which the fracture toughness is estimated.

- The fracture toughness was found to be $K_c = 3.12\ MPa.m^{1/2}$.

- The "Level 1" damage identification was a success using acoustic method and without any structural model.

- Positive mass (addition of mass) leads to mode (first) shift to lower range, while negative mass (crack) leads to mode shift to higher range.

- The last observation shows a very important enhancement of vibration-based analysis applied to fracture mechanism, as well as nondestructive evaluation

of thin material strength in presence of damage. Current results are expected to improvement in a quantitative manner.

## References


[1] Kao-Walter, S., Stahle, P., and Hagglund, R., *Fracture Toughness of a Laminate Composite* , in: Fracture of Polymers, Composites and Adhesives II, Elsevier, Oxford, UK, ISBN: 0-08-044195-5, 2002.

[2] Kao-Walter, S., Dahlstrom, J., Karlsson, T., and Magnusson, A., *A Study of Relation Between Mechanical Properties and Adhesion Level in a Laminated Packaging Material* , Mechanics of Composite Materials, Vol. 40, No.1, 2004.

[3] Lau, C. C., *A Fracture Mechanics Approach to the Adhesion of Packaging Laminates* , Doctoral Thesis, Imperial College of Science, UK, 1993.

[4] Tryding, J., *In Plane Fracture of Paper* , Division of Structural Mechanics, Lund university of Technology, 1996.

[5] Kao-Walter, S. and Stahle, P., *Mechanical and Fracture Properties of Thin Al-Foil* , Research report, Blekinge Institute of Technology, Sweden, 2001:09.

[6] Kao-Walter, S. and Stahle, P., *Fracture Behaviour of Thin Al-Foil - Measuring and Modelling of the Fracture Processes* , Submitted to "'Theoretical and Applied fracture Mechanics - Fracture Mechanics Technology"', 2004.

[7] Hagglund, R. and Stahle, P., *Tensile and Fracture Characterization of Tissue Paper Material* , Research Report, Malm University, 2001-07-24, Sweden.

[8] ASTM, *Standard test Methods for Plane Strain Fracture Toughness of Metallic Materials* , E399-90, 1990.

[9] Mothershead, J. E. and Frismell, M. I., *Model Updating in Structural Dynamics: a Survey* , Journal of Sound and Vibration, 167(2), pp 347-375, 1995.

[10] Fox, C. J., *The Location of Defects in Structures: A Comparison of the Use of Natural Frequency and Mode Shape Data* , in Proc. 10th IMAC, pp 522-528, 1992.

[11] Doeblin, S. W., Farar, C. and Prime, M., *A Summary Review of Vibration Based damage Identification methods* , The Schock and Vibr. digest, Vol.30, No.2, pp 91-105, 1998.

[12] Anderson, T. L., *Fracture Mechanics, Fundamentals and Applications* , 2nd edition, 1995.

[13] Mfoumou, E. and Kao-Walter, S., *Fracture Toughness Testing of Non Standard Specimens*, Research Report, Blekinge Institute of Technology, ISSN: 1103-1581, 2004.

# Paper B

# Vibration-Based Damage Detection and Evaluation of Sheet Materials using a Remote Acoustic Excitation

**Paper B is in review for journal publication as:**

Mfoumou, E., Hedberg, C., and Kao-Walter, S., “Vibration-Based Damage Detection and Evaluation of Sheet Materials using a Remote Acoustic Excitation”.

# Vibration-Based Damage Detection and Evaluation of Sheet Materials using a Remote Acoustic Excitation

Mfoumou, E. M., Hedberg, C. and Kao-Walter, S.

**Abstract**

A simple method of damage severity assessment on sheet materials is suggested and proved by theory and experiment. The investigated defect types are in forms of added mass and crack. The method is based on the frequency shift measurement of a material vibrating as a membrane subjected to static tension and irradiated by acoustic wave. It is shown both theoretically and experimentally that the natural frequency of the damaged membrane is shifted relative to its position in the ideal material. A local increase in thickness (or addition of mass) shifts the natural frequency down, while a crack shifts the frequency up. The method can be considered as acoustic weighing through the frequency shift. The sensitivity of this method can be high because frequency measurement is one of the most accurate measurements in physics and metrology.

*Keywords: Frequency shift, health monitoring, acoustic weighing.*

## 1 Introduction

The interest in the ability to monitor sheet materials and detect damage at the earliest possible stage is universal throughout the civil, mechanical, and aerospace engineering communities, where safety, reliability and quality control have a large impact on such materials' application fields. A well-known example is the laminate used for liquid food packages, which is made of several layers of thin sheets including polymer film, aluminum foil and paperboard. A defect in such a material will alter the mechanical properties of the package, having a great influence on the behavior and the functionality during its lifetime.

For the purposes of this paper, paperboard (100 $\mu$m thick) is investigated for damage severity assessment. Damage is defined in the forms of local increase in the material's standard thickness, and local separation in the material (without lost of mass). Implicit in this definition of damage is that the concept of damage is

not meaningful without a comparison between two different states of the material, one of which is assumed to represent the initial and undamaged state.

Most of the currently used damage identification methods belong to one of the following categories: visual or localized experimental methods such as acoustic or ultrasonic methods, magnetic field methods, radiography, eddy-current methods or thermal field methods [1]. All of these experimental techniques require that the vicinity of the damage is known a priori and that the portion of the material being inspected is readily accessible. The need for quantitative global damage detection methods has led to the development and continued research of methods that examine changes in the vibration characteristics of the structure. The usual approach of these methods consists in the determination of modal parameter changes due to the presence of the defect [2,3].

This paper is therefore a contribution to the advances of vibration-based technique by providing a firm mathematical and physical foundation to the issue related to the detection of inhomogeneity in sheet materials. It also confirms the high sensitivity of the frequency measurement in the field of physical measurements. Experiments and simulations are conducted to support the study. In the experimental part, a low frequency non-contact excitation with a loudspeaker is performed, and the response of the material is recorded through a laser Doppler vibrometer, while simulation is performed in a finite element code.

## 2 Vibration of membrane containing an added mass

### 2.1 Theory

In accordance with the conditions of the experiment described in Figure 1, consider the sample of paper as a membrane subjected to tension.

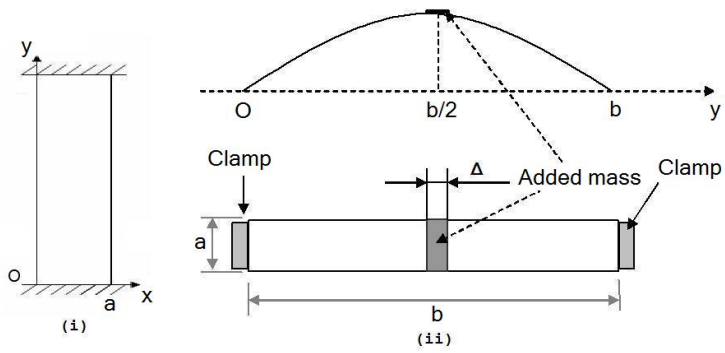


Figure 1: Specimen without (i) and with (ii) defect in form of added mass m'.

The equation of motion of the membrane, which lies in the plane of Cartesian coordinate system, has the form [4]:

$$\frac{\partial^2 \xi}{\partial t^2} - c^2 \left( \frac{\partial^2 \xi}{\partial x^2} + \frac{\partial^2 \xi}{\partial y^2} \right) = \frac{p\left(x, y, t\right)}{\rho h} \tag{1}$$

Here $\xi$ is the displacement of membrane along the z - axis from its equilibrium position z=0, $c = \sqrt{T/(\rho h)}$ is the velocity of propagation of bending wave which is determined by the tensile force $T$ per unit length of boundary of membrane, $\rho$ is the density and $h$ is the thickness of the membrane. The external pressure $p\left(x, y, t\right)$ is a function of time and of spatial coordinates. If the pressure is zero, the free vibration of a rectangular membrane can be represented as a series of natural modes:

$$\xi = \sum_{m,n=0}^{\infty} \xi_{mn} = \sum_{m,n=0}^{\infty} A_{mn} \cos\left( m\pi \frac{x}{a} \right) \sin\left( n\pi \frac{y}{b} \right) \sin\left( \Omega_{mn} t + \varphi_{mn} \right). \tag{2}$$

Here the constants $A_{mn}, \varphi_{mn}$ are amplitude and phase, $\Omega_{mn}$ is the natural frequency of mode,

$$\Omega_{mn} = c\sqrt{\left( \frac{\pi m}{a} \right)^2 + \left( \frac{\pi n}{b} \right)^2}, \quad m = 0, 1, 2, 3, ... \tag{3}$$

and $a, b$ are the dimensions of the membrane. Each mode in the solution (2) satisfies the boundary conditions

$$\xi_{mn}\left(x, y = 0\right) = 0, \quad \xi_{mn}\left(x, y = b\right) = 0, \quad \frac{d\xi}{dx}\left(x = 0, y\right) = 0, \quad \frac{d\xi}{dx}\left(x = a, y\right) = 0. \tag{4}$$

The conditions (4) correspond to the immovable boundaries at $y = 0, y = b$ and to the free boundaries at $x = 0, x = a$. If the membrane is loaded by an added mass $m'$ located at $x = x_0, y = y_0$, the behaviour of that mass is governed by the equation of motion

$$m' \frac{d^2 \xi}{dt^2} = -Sp\left(x, y, t\right), \tag{5}$$

where $S = l_1 l_2$ is the area of contact between the mass and membrane. The equation (1) with account for (5) has the following form:

$$\frac{\partial^2 \xi}{\partial t^2} - c^2 \left( \frac{\partial^2 \xi}{\partial x^2} + \frac{\partial^2 \xi}{\partial y^2} \right) = -\frac{m'}{\rho h S} \frac{\partial^2 \xi}{\partial t^2} \delta\left( \frac{x - x_0}{l_1} \right) \delta\left( \frac{y - y_0}{l_2} \right). \tag{6}$$

The Dirac $\delta$-functions are used here for simplicity, instead of continuous functions describing distribution of added mass on the surface of membrane. The $\delta$-function can be expanded in a Fourier series on the membrane modes:

$$\delta\left( \frac{x - x_0}{l_1} \right) = \frac{l_1}{a} + 2\frac{l_1}{a} \sum_{m=1}^{\infty} \cos\left( \pi m \frac{x_0}{a} \right) \cos\left( \pi m \frac{x}{a} \right), \tag{7}$$

$$\delta\left(\frac{y-y_0}{l_2}\right) = 2\frac{l_2}{b}\sum_{n=1}^{\infty}\sin\left(\pi n\frac{y_0}{b}\right)\sin\left(\pi n\frac{y}{b}\right). \tag{8}$$

It is necessary now to insert expansions (7), (8) and (2) into equation (6). For the modes $\xi_{0n}$ we get the dispersion law:

$$-\omega_{0n}^2 + c^2\left(\frac{\pi n}{b}\right)^2 = \frac{2m'}{M}\omega_{0n}^2\sin^2\left(\pi n\frac{y_0}{b}\right). \tag{9}$$

Here $M = \rho hab$ is the mass of membrane. Because $\Omega_0 n = \pi nc/b$ is the natural frequency of the unloaded membrane ($m' = 0$), the frequency of the loaded one will be different:

$$\omega_{0n} = \frac{\Omega_{0n}}{\sqrt{1+\frac{2m'}{M}\sin^2\left(\pi n\frac{y_0}{b}\right)}} \tag{10}$$

and for $m' << M$ we have

$$\omega_{0n} \approx \Omega_{0n}\left[1 - \frac{m'}{M}\sin^2\left(\pi n\frac{y_0}{b}\right)\right] \tag{11}$$

After the $\approx$ sign the simplified expression is written which is valid for loading mass small compared with the mass of membrane ($m' << M$). It follows from formula (11), that the frequency decreases with increase in loading. It depends also on the position of mass. If it is located in the maximum, the sine in (11) equals to unity and the frequency shift has its maximum. In the opposite case, if the mass $m'$ is located in the node, the sine is zero and the added mass does not influence the frequency of vibration.

For the general modes $\xi_{mn}, m \neq 0$, a different dispersion law is valid:

$$-\omega_{mn}^2 + c^2\left[\left(\frac{\pi m}{a}\right)^2 + \left[\left(\frac{\pi n}{b}\right)^2\right] = \frac{4m'}{M}\omega_{mn}^2\cos^2\left(\pi m\frac{x_0}{a}\right)\sin^2\left(\pi n\frac{y_0}{b}\right) \tag{12}$$

Consequently, the analog to formula (10) is

$$\omega_{mn} = \frac{\Omega_{mn}}{\sqrt{1+\frac{4m'}{M}\cos^2\left(\pi m\frac{x_0}{a}\right)\sin^2\left(\pi n\frac{y_0}{b}\right)}} \tag{13}$$

and for $m' << M$ we have

$$\omega_{mn} \approx \Omega_{mn}\left[1 - \frac{2m'}{M}\cos^2\left(\pi m\frac{x_0}{a}\right)\sin^2\left(\pi n\frac{y_0}{b}\right)\right] \tag{14}$$

The theory developed above offers an idea on how one can detect an inhomogeneity in form of added mass using a measurement of the frequency shift. In other words, we use "acoustic weighing" of the specimen. The frequency measurement is known to be one of most accurate physical measurement [5,6]. Consequently, one

can expect that the sensitivity of this method will be acceptable for nondestructive testing of sheet materials.

The sample studied is a rectangular strip of paper as shown in Figure 1. The addition of mass is a short strip of the same material, with the same width as the membrane. The strip is attached at the center of the membrane ($y = b/2$). The mode $\xi_{01}$ is excited by a loudspeaker. Consequently, the frequency shift is determined by formula (10):

$$\frac{\Omega_{01} - \omega_{01}}{\Omega_{01}} = 1 - \frac{1}{\sqrt{1 + \frac{2m'}{M}}} \tag{15}$$

For $m' << M$ we have

$$\frac{\Omega_{01} - \omega_{01}}{\Omega_{01}} \approx \frac{m'}{M} \tag{16}$$

For the mass of the specimen being small in comparison with the mass of membrane, the relative shift equals to the ratio of these masses.

## 2.2 Experiment

The case study investigated in this work is a single layer material (paperboard) clamped at the upper and lower edges in a tensile test machine, making the edges immovable (nodes). As a membrane has no compression or bending stiffness, it must be pre-stressed in order to act as a structural element. Therefore, the specimen is slightly loaded (within its elastic region) just enough to produce bending waves from a periodical acoustic load.

The specimen is preloaded at *17 N* and has a mean thickness of $h = 0.1$ *mm*. The length is $b = 650$ *mm* and the width is $a = 12$ *mm*. The acoustic load is provided by a loudspeaker having *4-8 Ohm* impedance, and a broad frequency range of *70* to *20.000 Hz*, centered at the middle of the specimen. Using an Agilent function generator the excitation frequency can be tuned continuously. A picture of the experimental setup is shown in Figure 2.

The specimens are excited using a *10 V* sine sweep signal between *0* and *900 Hz*, which is sent to the loudspeaker through a function generator. The middle of the specimen is chosen as region of excitation, leading to strong excitation of odd modes of vibration. The method is to monitor the amplitude of the signal received in the time domain by a VS-100 OMETRON laser vibrometer, using A scans at the middle of the material. The laser signal fed to a high-pass/low-pass filter assures that only the excited frequency range is included in the velocity reading.

Small strips of mass *12 mg* (*2.25%* of the total mass of the specimen) are successively added to the middle of the specimen length. The fundamental frequency

shift is monitored for 1-10 added strips.

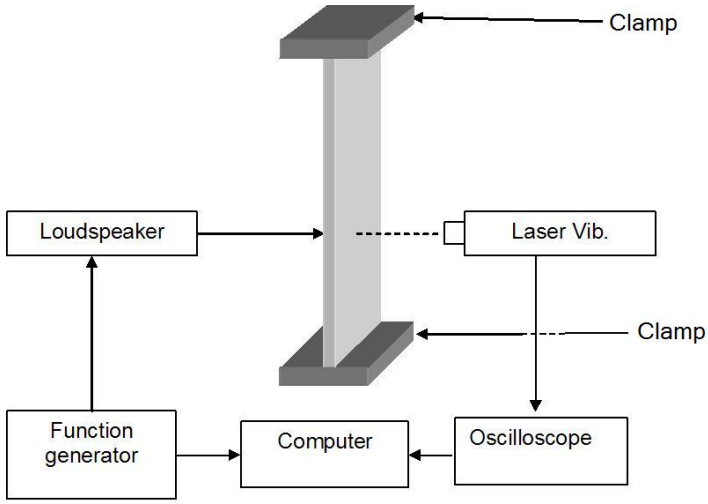


Figure 2: Experimental configuration.

## 2.3 Results

By inducing a defect in form of added mass the dominant fundamental eigenfrequency shifts to the left because the frequency is inversely proportional to the square root of the mass, as shown in equation (10). Table 1 shows the calculated fundamental frequency corresponding to the undamaged specimen, and illustrates the experimentally observed frequency shifts of the fundamental mode with addition of a mass corresponding to 2.25% of the total mass of the membrane.

| | Theory | Experiment |
|---|---|---|
| Intact | 110.7 | 108.21 |
| Damaged | 108 | 105 |

Table 1: Fundamental frequencies for intact and damaged specimens.

A good agreement is obtained between the analytical (equation (15)) and experimental results, for a defect located at the middle of the specimen. This can be seen for the first mode resonance peak shift in Figure 3.

The variation tends to be somewhat nonlinear with increasing mass, showing that some nonlinear dependence has to be taken into account.

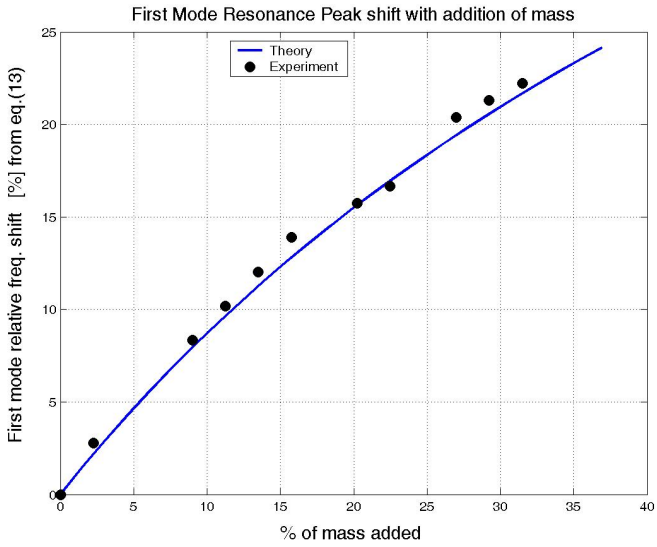


Figure 3: First mode relative frequency shift with addition of mass.

# 3 Vibration of membrane containing a mass deficiency (crack)

## 3.1 Theory

Let the membrane contain a crack as shown in Figure 4. Such a defect can be considered as a local opening in the material without reduction of the global mass of the structure.

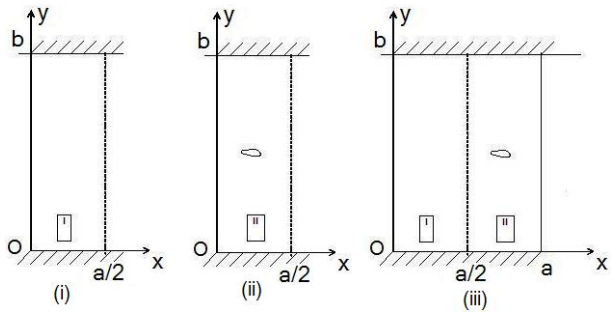


Figure 4: Specimen configuration for hand-made small defect.

The membrane consists of two sections of equal width but with different velocities of bending waves. If these sections are *isolated* and *vibrate independently*

their motions are governed by two different equations like (1):

$$\frac{\partial^2 \xi^{(1,2)}}{\partial t^2} - c_{1,2}^2 \left( \frac{\partial^2 \xi^{(1,2)}}{\partial x^2} + \frac{\partial^2 \xi^{(1,2)}}{\partial y^2} \right) = 0 \tag{17}$$

Index 1 here corresponds to the left (figure 4-(i)), and 2 - to the right-hand (figure 4-(ii)) section. Let the membranes vibrate in the $\xi_{m1}$ mode. The solutions to (17) are

$$\xi^{(1,2)} = A^{(1,2)}(x) \sin\left(\pi \frac{y}{b}\right) \cos\left(\omega^{(1,2)} t\right) \tag{18}$$

If $A^{(1,2)}(x) = \cos(m\pi x/a)$ , the natural frequencies are equal to

$$\omega_{m1}^{(1,2)} = \sqrt{\left(\frac{\pi}{b} c_{1,2}\right)^2 + \left(m \frac{\pi}{a} c_{1,2}\right)^2} \tag{19}$$

Substituting (18) into (17) we derive:

$$\frac{d^2 A^{(1,2)}}{dx^2} + \left( \frac{\omega^{(1,2)2}}{c_{1,2}^2} - \frac{\pi^2}{b^2} \right) A^{(1,2)} = 0 \tag{20}$$

In case $A^{(1,2)}(x) = const$, we have the fundamental mode for which $\omega^{(1,2)} = (\pi/b)\, c_{1,2}$. Let $c_2 < c_1$ and, consequently, $\omega_2 < \omega_1$.

If the two sections of the membrane are *joined* (figure 4-(iii)), they vibrate with the frequency $\omega$, which lies between $\omega_2$ and $\omega_1$:

$$\omega_2 < \omega < \omega_1 \tag{21}$$

We now seek the solutions of equations (17) in the form:

$$\xi^{(1,2)} = A^{(1,2)}(x) \sin\left(\pi \frac{y}{b}\right) \cos(\omega t) \tag{22}$$

where $\omega$ is an unknown frequency. Substituting (22) into (17), we obtain:

$$\frac{d^2 A^{(1)}}{dx^2} + \left( \frac{\omega^2}{c_1^2} - \frac{\pi^2}{b^2} \right) A^{(1)} = 0 \tag{23}$$

$$\frac{d^2 A^{(2)}}{dx^2} + \left( \frac{\omega^2}{c_2^2} - \frac{\pi^2}{b^2} \right) A^{(2)} = 0 \tag{24}$$

The coefficients in front of $A^{(1,2)}$ have different signs. In fact:

$$\frac{\omega^2}{c_1^2} - \frac{\pi^2}{b^2} = \frac{\omega^2}{c_1^2} - \frac{\omega_1^2}{c_1^2} < 0, \quad \frac{\omega^2}{c_2^2} - \frac{\pi^2}{b^2} = \frac{\omega^2}{c_2^2} - \frac{\omega_2^2}{c_2^2} > 0 \tag{25}$$

The inequalities (25) are valid because the ratio (21) between the frequencies exists. Consequently, equations (23) and (24) can be rewritten as follow:

$$\frac{d^2 A^{(1)}}{dx^2} - k_1^2 A^{(1)} = 0, \quad \frac{d^2 A^{(2)}}{dx^2} - k_2^2 A^{(2)} = 0 \tag{26}$$

with

$$\kappa_1^2 = \frac{\pi^2}{b^2} - \frac{\omega^2}{c_1^2}, \quad \kappa_2^2 = \frac{\omega^2}{c_2^2} - \frac{\pi^2}{b^2} \tag{27}$$

The well-known solutions to equations (24) are

$$A^{(1)} = \alpha_1 \cosh(\kappa_1 x) + \beta_1 \sinh(\kappa_1 x) \tag{28}$$

$$A^{(2)} = \alpha_2 \cos(\kappa_2 x) + \beta_2 \sin(\kappa_2 x) \tag{29}$$

$\alpha_1, \alpha_2, \beta_1$ and $\beta_2$ are constants.

Solving $\frac{dA^{(1)}}{dx}|_{x=0} = 0$ and $\frac{dA^{(2)}}{dx}|_{x=a} = 0$ for $\beta_1$ and $\beta_2$ and substituting into (26) and (27) leads to the simpler forms:

$$A^{(1)} = \alpha_1 \cosh(\kappa_1 x) \tag{30}$$

$$A^{(2)} = \alpha_2 \frac{\cos(\kappa_2 a - x)}{\cos(\kappa_2 a)} \tag{31}$$

Solutions (30) and (31) must now be sewed at *x=a/2* and we have:

$$A^{(1)}(x = a/2) = A^{(2)}(x = a/2) \Rightarrow \alpha_1 \cosh\left(\kappa_1 \frac{a}{2}\right) = \alpha_2 \frac{\cos\left(\kappa_2 \frac{a}{2}\right)}{\cos(\kappa_2 a)} \tag{32}$$

and

$$\frac{dA^{(1)}}{dx}|_{x=a/2} = \frac{dA^{(2)}}{dx}|_{x=a/2} \Rightarrow \alpha_1 \kappa_1 \sinh\left(\kappa_1 \frac{a}{2}\right) = \alpha_2 \kappa_2 \frac{\sin\left(\kappa_2 \frac{a}{2}\right)}{\cos(\kappa_2 a)} \tag{33}$$

The ratio of equations (32) and (33) leads to the following dispersion law:

$$\kappa_1 \tanh\left(\kappa_1 \frac{a}{2}\right) = \kappa_2 \tan\left(\kappa_2 \frac{a}{2}\right) \tag{34}$$

For the fundamental mode, for $\kappa_1 \frac{a}{2} << 1$ and $\kappa_2 \frac{a}{2} << 1$, $\tanh\left(\kappa_1 \frac{a}{2}\right) \approx \kappa_1 \frac{a}{2}$, $\tan\left(\kappa_2 \frac{a}{2}\right) \approx \kappa_2 \frac{a}{2}$,

and we have: $\kappa_1^2 = \kappa_2^2$

From definitions (27) we get:

$$\omega^2 = 2 \frac{\pi^2}{b^2} \frac{c_1^2 c_2^2}{c_1^2 + c_2^2} \tag{35}$$

Equation (35) gives the fundamental frequency of a membrane consisting of two different sections of equal size.

Assuming $c_1^2 \approx c_2^2$ with $c_1 \equiv c$ and $c_2 \equiv c(1 - \delta)$, $\delta << 1$, we obtain the following frequency:

$$\omega = \omega_1 \left(1 - \frac{c_1 - c_2}{2c_1}\right) \tag{36}$$

If $c_2 < c_1$ (which is the case on the configuration in figure 4), the frequency shifts down, and the absolute value of the relative frequency shift is:

$$\frac{\omega - \omega_1}{\omega_1} = -\frac{c_1 - c_2}{2c_1} \tag{37}$$

### 3.2 Experiment

The experimental setup is similar to the previous one in (2.2), with the defect configuration on the specimen as shown in Figure 4. The defect is hand-made in form of crack with a sharp knife, in the width direction; its length is *2 mm*. No material is removed. The specimen is preloaded at *14 N* and has a mean thickness of $h = 0.1$ *mm*. The length is $b = 550$ *mm* and the width is $w = 12$ *mm*. As an unloaded membrane has no bending stiffness, it is pre-stressed in order to act as a structural element.

The excitation frequency range is *70-500 Hz*, with an *8 Vpp* sine sweep. The amplitude of the membrane vibration is recorded at the mid-point with the VS-100 OMETRON laser vibrometer.

A frequency analysis with FFT is performed on the received signal. A Hanning window (Von Hann) is applied to reduce leakage and improve amplitude accuracy. The record length is *1kS* at a rate of *2 kS/s*. A leastPrime algorithm is used to display the power spectrum of the signal.

### 3.3 Results

The resonance peak responses for specimen with and without crack are recorded at increasing frequency drive level. An illustration of the frequency response of the material behavior is shown on Figure 5.

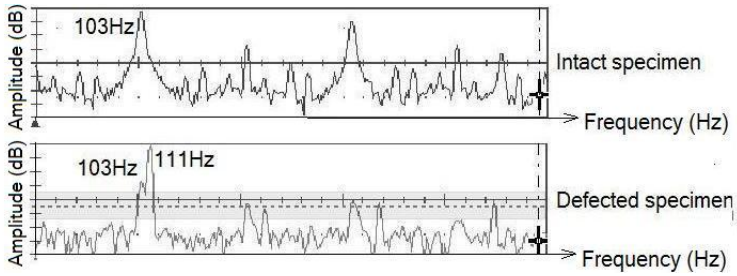


Figure 5: Frequency sweep response. A new peak appears when damage is introduced.

A second spectral line (111 Hz) appears in the damaged case. It is the scatterer introduced in form of a crack that generates an additional spectral line. This agrees with the prediction in the analytical study. Meanwhile, the new spectral line is unstable in height, exact location and existence, revealing that this new feature (in the spectrum) may be connected to the randomly opening and closing of the defect. Such unstable behaviour of crack was observed recently at vibration of a metallic disk [7]. It was discovered that a crack starts to vibrate in a very narrow

range of both amplitude and frequency of the incident wave. After several periods of vibration the corresponding spectral line disappears, and then appears again (see also [8]).

Qualitatively, we therefore observe a duplication of frequency at the fundamental mode as derived in the theoretical part. The table below summarizes the results.

| | Intact | Damaged (mixing) | Damaged (no mixing) |
|---|---|---|---|
| Theory | 118 | 115.7 | 118 and 115.7 |
| Experiment | 103 | 103 and 111 | - |

Table 2: Fundamental frequencies for intact and damaged specimens with and without frequency mixing.

# 4 Finite Element Modeling

## 4.1 Problem description, geometry and model

Rectangular membranes with and without defect were investigated for natural frequency extraction. The finite element code ABAQUS 6.5 [9] was used to verify the analytical and experimental results. The specimen dimensions and material properties were those given previously.

In the analysis, linear elastic behavior and membrane elements were used to model the material. Membrane elements are used to represent thin surfaces in space that offer strength in the plane of the element but have no bending stiffness. On the other hand, for thin-membrane behavior, the transverse shear and rotary inertia were neglected and an isotropic material behavior was assumed. In this case, only Young's modulus and Poisson's ratio were needed. The element type M3D4R was used to model the material. This is a three-dimensional four-node membrane element with reduced integration, often used for crack meshes problems. However, additional mesh refinement was needed around the defect zone. Reduced integration provides accurate results at a significantly less running time.

The defect in form of a crack was represented as a local deficiency of mass with negligible mass lost compared to the total mass of the material. The corresponding mesh is shown in Figure 6. The defect severity was modeled by moving the nodes at the tips, hence increasing the crack length $a_0$, which led to a deformation in connected elements and thus, to a local change in the elements stiffness.

The so-called virtual crack extension approach [10] was used in ABAQUS.

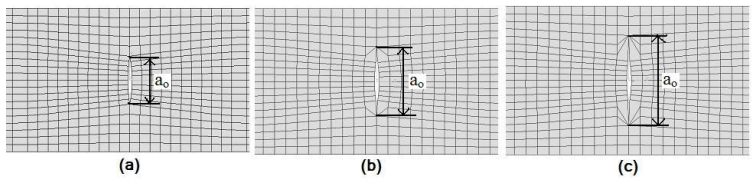


Figure 6: Mesh around the defect in the FE model. Crack lengths (a):$a_0 = 3.5mm$ (b):$a_0 = 4.6mm$ (c):$a_0 = 5.7mm$

One of the methods used, the stiffness derivative formulation [11], is a finite element method for inferring energy release rate in bodies. From this formulation, a subsequent work may show that the energy release rate, which is shown to be proportional to the derivative of the stiffness matrix of the material, can be used in this study as a damage indicator.

The defect in form of added mass was modeled as a local increase in thickness on a set of elements covering the defected area, as illustrated in figure 7.

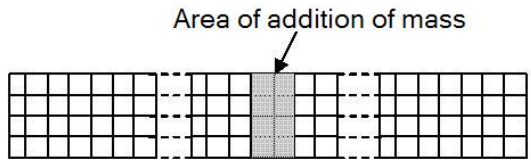


Figure 7: Meshed membrane with an area illustrating an increase in local density of the material.

An eigenvalue analysis was performed with a *Frequency* step, for natural frequency extraction using the Lanczos eigensolver. The boundary condition was defined as specified on the theoretical model.

The dissipation of energy is caused by a number of effects, including friction at the separated faces of the material (crack) and other localized material hysteresis. Damping is a convenient way of including the important absorption of energy without modeling the effects in detail. In ABAQUS/Standard the eigenmodes are calculated for the undamped system, yet most engineering problems involve some kind of damping, however small. This may explain the deviation observed between simulation and experimental or analytical results.

## 4.2 Results

The Figures 8 a-b show that scattering introduction, either in form of added mass or in form of crack, shifts the fundamental frequency, and the relative frequency

shift versus percentage of added mass, and normalized crack length has the same trend as observed both in theoretical and experimental parts. The fundamental frequency decreases because, the frequency being inversely proportional to the square root of the mass, locally increasing the mass will shift the fundamental frequency to the left. In case of a crack the frequency shifts to the left as well.

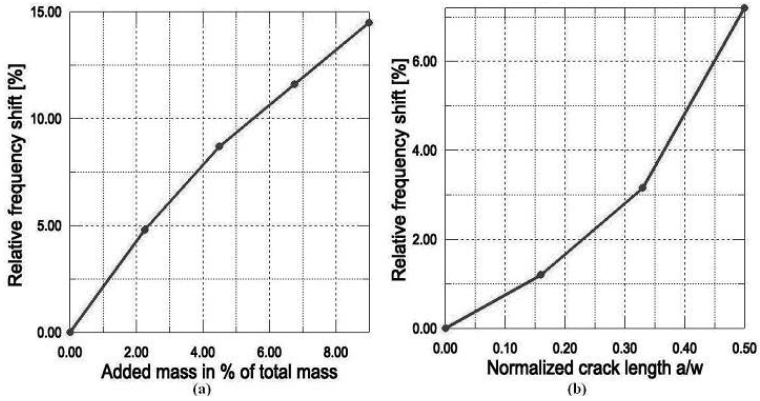


Figure 8: Fundamental frequency shift vs. defect severity for (a):addition of mass; and (b):crack.

# 5 Conclusions

In general, non-destructive testing using vibration-based methods employ natural frequencies, bending modes, resonant frequencies, appearance of new features in the spectral response, and the width of peaks in the frequency spectrum as well as acoustical impedance. These effects are related to mechanical properties such as velocity, stiffness, density or damping, that are important for the integrity of the material. Local changes in mechanical properties that might be related to potential defects cause changes in the measured values and therefore induce shifts of resonance frequencies or broadening of peaks (damping). Results are achieved by comparing the measured values with those of a "healthy" reference material.

This issue is successfully proven in this work. A theoretical model is derived, which qualitatively illustrates the duplication of frequency by a crack, observed from experimental results, for sheet materials. In case of crack, and at low frequency modes, it is difficult to experimentally observe this damage signature, because as stated in previous work [Doebling et. Al.], the natural mode shapes mask the local vibration pattern introduced by the defect. However, a noticeable frequency shift is observed from our results, making the approach useful for damage

assessment in such materials. A similar observation was recently made on a homogeneous rectangular membrane with different kinds of restraints on different sides [12]. It was observed that a decrease in the natural frequency of a membrane indicates a defect in the membrane fastening. Because of standing wave fields and nodes for a single mode, there is no constant sensitivity over the entire material and defects may not be found sometimes. In that case, the nodes have to be well identified and more than one mode will be measured. In general, the theory developed is convenient for applications such as evaluation of the standard thickness deviations of membranes.

This paper also shows the sensitivity of acoustic weighing for nondestructive testing of sheet materials. The derived theory together with the experiments conducted show how inhomogeneities in form of added mass can be detected using measurement of the frequency shift. Indeed, from equation (16) it is possible to infer that for a membrane vibrating at about *110 Hz*, a mass sensitivity $\Delta f/m'$ of the order of *0.25 Hz/mg* can be considered possible. Meanwhile, the damage may not show up in all but only in some mode shapes. Therefore, the mode-dependent energy dissipation at the defected zone can be revealed by monitoring higher modes, which will lead to the sensitivity of the approach all over the material. The theory developed in this paper is also an accurate tool for that purpose.

## Acknowledgement

The authors are thankful to Prof. I. Yu. Solodov for valuable discussions during the visit of one of the co-authors (E. Mfoumou) at the Institute for Polymer Testing and Polymer Science (IKP) in Stuttgart, Germany. We would also like to give our utmost thanks to Professor O. V. Rudenko from Moscow State University, Russia, for his contribution to this work.

## References

[1] Doherty, J.E., *Nondestructive Evaluation*, Chapter 12 in Handbook on Experimental Mechanics, A. S. Edt, Society for Experimental Mechanics, inc. 1988.

[2] Doebling, S.W., Farrar, C.R., and Prime, M.B., *Summary Review of Vibration-Based Damage Identification Methods*, Shock and Vibration Digest, 30 (2), 91-105. 1998.

[3] Hagemaier, D.J. and Fassbender, R.H, *Nondestructive testing of advanced composites*, Materials Evaluation 37 pp 43-49(1979).

[4] Landau L.D., and Lifshitz E.M., *Theory of Elasticity*, 3rd Edition, Pergamon, 1979.

[5] Sauerbrey, G., *Use of Vibrating Quartz for Thin Film Weighting and Microweighting*, (in German), Z. Phys., 155, 206-222, 1959.

[6] King, W. H., *Piezoelectric Sorption Detector*, Anal. Chem., 36 (9), 1735-1739, 1964.

[7] Korobov, A. I., Izosimova, M. Yu, *Nonlinear Lamb Waves in a Metallic Plate Containing Defects*, Acoustical Physics, Vol. 52, No. 3, 2006.

[8] Rudenko, O. V., *Giant Nonlinearities of Structurally-inhomogeneous Media and Principles of Nonlinear Acoustic Diagnostics (a review)*, Physics-Uspekhi (Advances in Physical Sciences), Vol. 176, No.1, pp. 77-95, 2006.

[9] ABAQUS/Standard User's Manual. Volume I-III Version 6.5, Hibbit, Karlsson and Sorensen, Inc., 2004.

[10] Hellen, T.K., *On the Method of Virtual Crack Extensions*, International Journal for Numerical Methods in Engineering, Vol. 9, pp. 187-207, 1975.

[11] Parks, D.M., *A Stiffness Derivative Finite Element Technique for Determination of Crack Tip Stress Intensity Factors*, International Journal of Fracture, Vol. 10, pp. 487-502, 1974.

[12] Akhtyamov, A. M., *Identification of the Boundary Conditions of a Rectangular Membrane from its Natural Frequencies*, Acoustical Physics, Vol. 52, No. 3, 2006.

# Paper C

# Acoustical Measurement Accompanying Tensile Test: New Modality for Non Destructive Testing and Characterization of Sheet Materials.

**Paper C is published as:**

Mfoumou, E., Rudenko, O.V., Hedberg, C., and Kao-Walter, S., "Acoustical Measurement Accompanying Tensile Test: New Modality for Non-Destructive Testing and Characterization of Sheet Materials". *CD-ROM Proceedings of the 13th International Congress on Sound and Vibration (ICSV13)*, July 2-6, 2006, Vienna, Austria, Eds.: Eberhardsteiner, J.; Mang, H.A.; Waubke, H., Publisher: Vienna University of Technology, Austria, ISBN: 3-9501554-5-7

# Acoustical Measurement Accompanying Tensile Test: New Modality for Non-Destructive Testing and Characterization of Sheet Materials

Mfoumou, E., Rudenko, O., Hedberg, C., and Kao-Walter, S.

**Abstract**

A series of uniaxial tensile tests was performed for sheet materials like paperboard, polyethylene and packing layered composites. These sheets can be considered as membranes. In parallel with a tensile test, the natural frequency was measured through an acoustical excitation.

Firstly, it was shown both theoretically and experimentally that, at a given load, the frequency is sensitive to the local deviation in the standard thickness or to the presence of cracks inside the material. It means that this acoustic measurement can be used as one of the methods of damage assessment, or nondestructive testing in general.

Secondly, the resonance frequency shift was continuously monitored for increasing strain on polyethylene and paperboard, and the curves obtained were compared to the stress-strain curves for material characterization. They were not the same and showed a non-monotonic stiffness variation for the polyethylene. It was shown that the resonance frequency shift correlates with the stress-strain curve for material characterization under tensile test.

*Keywords: Acoustical measurement, material characterization, frequency shift, vibration-based, damage severity.*

## 1 INTRODUCTION

Materials characterization is important to perform failure analyses on samples. Samples can be analyzed to determine the failure mode, and solutions to prevent further problems. Meanwhile, Fracture Mechanics methodology has strongly indicated the importance of nondestructive (NDT) as a decision-supporting tool [1].

A previous work [2] has considered vibration-based technique by providing a firm mathematical and physical foundation to the issue related to defect detection in sheet materials. It was shown that the presence of a scaterrer in form of crack shifts the resonance frequency of the material. As a matter of fact, it seemed important to investigate the quantitative aspect of this observation, by studying the variation of the resonant frequency with an increase in defect severity, which is within the frame of this paper.

Different nondestructive methods are used for material characterization [3]. The dynamic response through a non-contact vibration-based technique is used in this study to investigate some phenomena accompanying elastic and plastic deformations on paperboard and LDPE, such as the resonant frequency shift. Beforehand, the mechanical properties of materials are determined in tensile testing, using a destructive method. The specimen under investigation, held by clamps, is subject to mechanical loading until rupture. However, there are relationships between mechanical properties and modal parameters, specifically the resonance frequency. It is well known that for a specimen under tension, the frequency is proportional to the speed of the transversal wave propagating along the material, which in turn is related to the remote stress,thus to the rigidity of the material. The changes in the material structural integrity may then be detected by a non-contact vibration-based technique. Hence, this method may be used to determine the physical and mechanical properties of materials.

# 2 DAMAGE SEVERITY ASSESSMENT ON PAPERBOARD

## 2.1 Theory

Consider the sample of paperboard in Figure 1 as a membrane subjected to tension (i) and transversal acoustical excitation (ii).

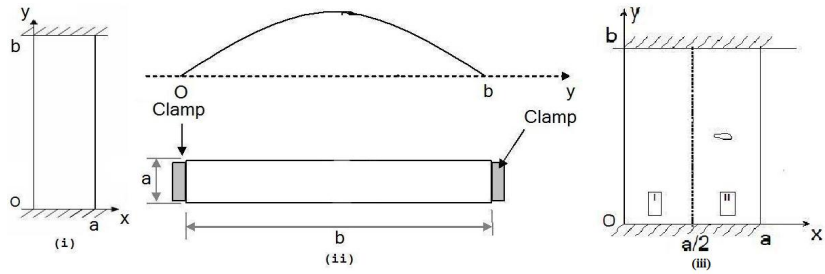


Figure 1: Specimen configuration.

The equation of motion of the membrane without account of external pressure, has the form [4]:

$$\frac{\partial^2 \xi}{\partial t^2} - c^2 \left( \frac{\partial^2 \xi}{\partial x^2} + \frac{\partial^2 \xi}{\partial y^2} \right) = 0 \tag{1}$$

where $\xi$ is the displacement of membrane along the z - axis from its equilibrium position z=0, $c = \sqrt{T/(\rho h)}$ is the velocity of propagation of bending wave which is determined by the tensile force $T$ per unit length of boundary of membrane, $\rho$ is the density and $h$ is the thickness of the membrane. The free vibration of a rectangular membrane can then be represented as a series of natural modes:

$$\xi = \sum_{m,n=0}^{\infty} \xi_{mn} = \sum_{m,n=0}^{\infty} A_{mn} \cos\left( m\pi \frac{x}{a} \right) \sin\left( n\pi \frac{y}{b} \right) \sin\left( \omega_{mn} t + \varphi_{mn} \right). \tag{2}$$

where the constants $A_{mn}$ and $\varphi_{mn}$ are amplitude and phase, $\omega_{mn}$ is the natural frequency of the mode,

$$\omega_{mn} = c\sqrt{\left( \frac{\pi m}{a} \right)^2 + \left( \frac{\pi n}{b} \right)^2}, \quad m = 0, 1, 2, 3, ... \tag{3}$$

and $a, b$ are the dimensions of the membrane. Each mode in the solution (2) satisfies the boundary conditions

$$\xi_{mn}(x, y = 0) = 0, \quad \xi_{mn}(x, y = b) = 0, \quad \frac{d\xi}{dx}(x = 0, y) = 0, \quad \frac{d\xi}{dx}(x = a, y) = 0. \tag{4}$$

The conditions (4) correspond to immovable boundaries at $y = 0, y = b$ and to free boundaries at $x = 0, x = a$.

Let the membrane contain a crack as shown in Figure 1-(iii). It consists of two sections of equal width but with different velocities of bending waves. If these sections are isolated and vibrate independently their motions are governed by two different equations like (1):

$$\frac{\partial^2 \xi^{(1,2)}}{\partial t^2} - c_{1,2}^2 \left( \frac{\partial^2 \xi^{(1,2)}}{\partial x^2} + \frac{\partial^2 \xi^{(1,2)}}{\partial y^2} \right) = 0 \tag{5}$$

Index 1 here corresponds to the left hand section, and 2 to the right-hand section. Let the membranes vibrate in the $\xi_{m1}$ mode. If the two sections of the membrane are joined, they vibrate with the frequency $\omega$, which lies between $\omega_2$ and $\omega_1$:

$$\omega_2 < \omega < \omega_1 \tag{6}$$

and the solutions to (5) are in the form:

$$\xi^{(1,2)} = A^{(1,2)}(x) \sin\left( \pi \frac{y}{b} \right) \cos(\omega t) \tag{7}$$

where $\omega$ is an unknown frequency.

From the previous equations, it is shown [Mfoumou et. al.] that the fundamental frequency of the membrane consisting of two different sections of equal size is given by

$$\omega = \omega_1 \left(1 - \frac{c_1 - c_2}{2c_1}\right) \tag{8}$$

And if $c_2 < c_1$, the frequency shifts down, and the absolute value of the relative frequency shift is:

$$\frac{\omega - \omega_1}{\omega_1} = -\frac{c_1 - c_2}{2c_1} \tag{9}$$

## 2.2 Experiment

The experimental setup is shown in figure 2. A cracked panel as illustrated in Figure 1-(iii) is considered. The 2 mm long crack is cut manually using a razor blade. The width and length of the specimen are w=30 mm and L=550 mm. The paperboard used has a thickness h=100 $\mu m$.

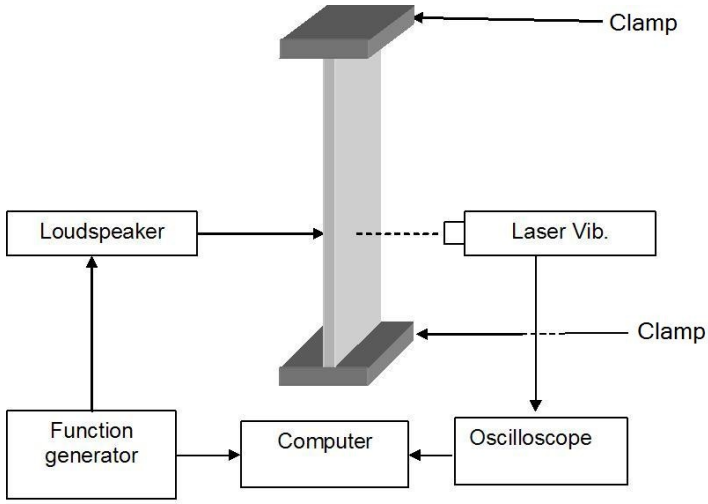


Figure 2: Experimental configuration.

The test is made on a MTS Universal Testing Machine with a 100N loadcell. A pair of pneumatic clamps are used to hold the specimen. The specimen is vertically positioned between the upper and lower clamps, and is increasingly loaded until a load of 16N is reached. The MTS software TextWorks is used to monitor the loading process. The test is performed at a room temperature of $23^oC$ and 40% humidity, at a cross-head speed of 5mm/min.

The specimen is transversaly excited using a 8Vpp sine signal through a loudspeaker and the second bending mode (on the length direction) is monitored for increasing crack length. A VS-100 OMETRON laser vibrometer is used for sensing of vibrations from the material. In parallel, the updated load resulting from the material softening due to the increase in crack length is continuously recorded from the TestWorks display panel.

### 2.3 Results and correlation

It was shown [Mfoumou et. al.] that the resonance frequency shifts down by introduction of a defect in form of crack. As a matter of fact, the frequency continuously decreases due to the increase in crack length, and monitoring of the third bending mode shows a good agreement between experimental and analytical results, as shown in Figure 3.

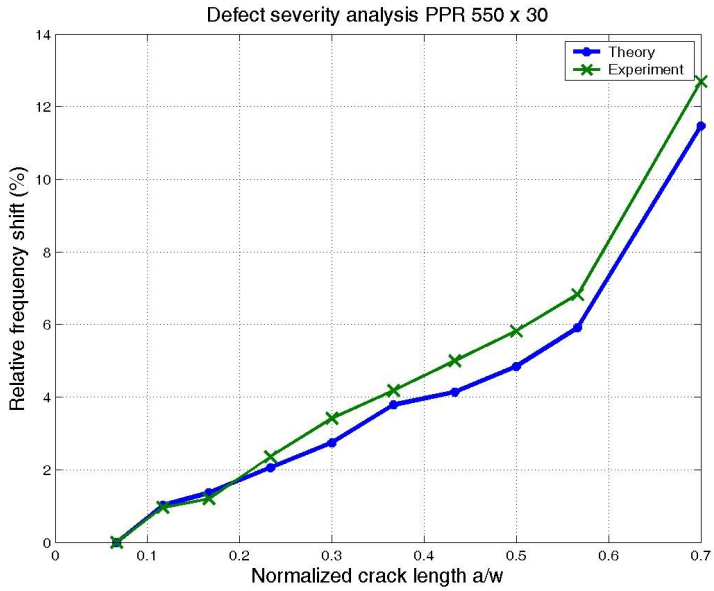


Figure 3: Third mode relative frequency shift[equation(9)] with defect severity.

# 3 ACOUSTICAL MEASUREMENT FOR MATERIAL CHARACTERIZATION

## 3.1 Standard mechanical characterization

The tensile test is widely used to provide basic information on the strength of materials and as an acceptance test for the specification of materials. In the tensile test the specimen is subjected to a continually increasing uniaxial tensile force while simultaneous observations are made of the elongation of the specimen.

Two rectangular strips - one of paperboard and one of polyethylene - are considered. The densities and sizes of the materials are specified on table 1.

| Material | Density (g/cm$^3$) | Length (cm) | Width (cm) | Thickness ($\mu m$) |
|---|---|---|---|---|
| PPR | 0.684 | 55 | 3 | 100 |
| LDPE | 0.91 | 10 | 1.5 | 27 |

Table 1: Materials under investigation.

The same equipment as in the previous case is used. The specimen is increasingly loaded by moving the crosshead up. The test is performed under displacement control at a cross-head speed of 0.5 mm/min for the plastic and 0.07 mm/min for paperboard. An engineering stress-strain curve is then constructed from the load/elongation measurements and is illustrated in Figures 4a-b both for paperboard and LDPE.

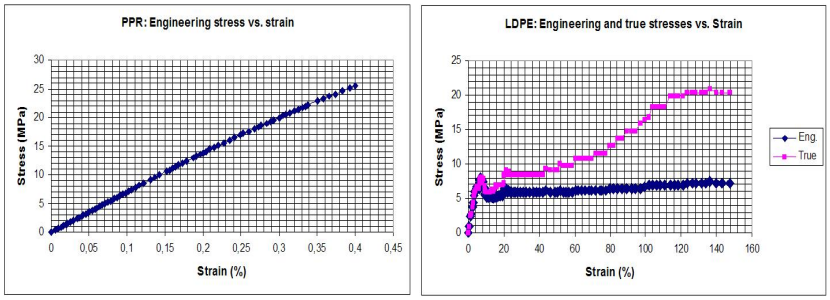


Figure 4: The stress-strain curves from standard tensile test.

## 3.2 Acoustic measurement

In parallel with the tensile test, the specimen is transversaly excited with a loudspeaker. A reference frequency corresponding to one resonance frequency of the

material is considered within the elastic region of the stress-strain curve. That resonance frequency is shifting with increase in strain, and the characteristic curves are plotted in Figure 5a-b.

The general shapes of the frequency-strain curves in Figure 5 require further explanation. For both materials, the second mode resonance frequency is monitored. In the elastic region, the load increases, and the resonance frequency is proportional to the square roots of strain and elastic modulus. When the load exceeds a value corresponding to the yield strength, the specimen undergoes strong plastic deformation. Further details are given below.

The observations made so far lead to the conclusion that the stress-strain curve correlates with the frequency-strain curve for material characterization.

### 3.3 Analysis

Consider the general expression of resonance frequencies given in equation (3). As the mode numbers $m$ and $n$ being constant for a given resonance frequency, it follows that the resonance frequency is proportional to the transversal wave velocity:

$$\omega_{mn} = \alpha\sqrt{\frac{F}{\rho a h}} \tag{10}$$

where $F$ is the applied load and $\alpha = \sqrt{\left(\frac{\pi m}{a}\right)^2 + \left(\frac{\pi n}{b}\right)^2}$.

It can also be demonstrated that the previous equation can be rewritten as follows:

$$\omega_{mn} = \alpha\sqrt{\frac{\sigma}{\rho}} \tag{11}$$

where $\sigma$ represents the remote stress that elongates the specimen.

For the second bending mode, $m = 0$, $n = 2$, we have $\alpha = \frac{2\pi}{b}$. It follows that

$$\omega_{mn} = \frac{2\pi}{b}\sqrt{\frac{\sigma}{\rho}} = \alpha\sqrt{\frac{E\epsilon}{\rho}} \tag{12}$$

Figures 5a-b show the plots of analytical (equation 12) and experimental results. An acceptable agreement is obtained, and besides, the shapes of the curves are more illustrative than those of tensile tests.

In equation 12, the resonance frequency is linearly proportional to the square root of the strain and thus, shifts up with increase in strain. When the material enters the plastic region, the Young's modulus starts (in principle) to decrease.

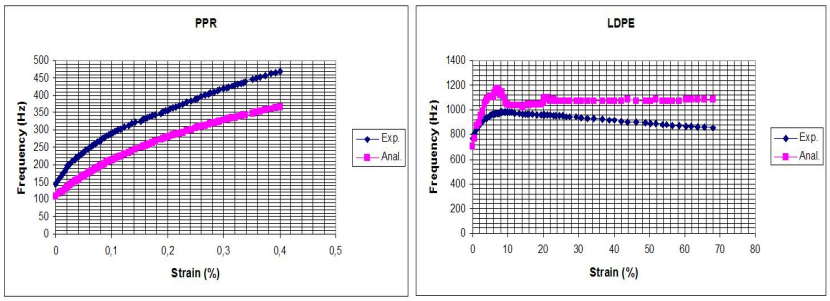


Figure 5: Analytical and experimental frequency-strain curves.

However, the stress to produce continued plastic deformation increases with increasing strain, i.e., the materials strain-harden. The volume of a specimen remains constant during plastic deformation, and as the specimen elongates, it decreases uniformly along the gauge length in cross-sectional area.

Initially the strain hardening more than compensates for this reduction in Young's modulus, and the frequency (proportional to square root of strain) continues to rise with increasing strain. Eventually a point is reached where the decrease in stiffness is greater than the strain hardening. Because the stiffness now is decreasing far more rapidly than strain hardening, the actual load required to deform the specimen falls off and the resonance frequency likewise decreases until fracture occurs.

# 4 CONCLUSION

The issue related to low frequency acoustic measurement for damage severity assessment is proven in this work with a good accurary. A previous work [Mfoumou et. al] has shown that the resonance frequency shifts down with introduction of a crack in the material. As a continuation, this work correlates the analytical and experimental variation of the resonance frequency with an increase in the defect severity, with a good agreement. Therefore, the low frequency investigation of the vibration-based technique is sensitive to changes in standard thickness or crack inside the material.

More importantly, the possible connectivity of the standard mechanical testing (Fracture Mechanics) to remote acoustical measurement (NDT) is successfully proven for material characterization in this work. It is successfully shown that the resonance frequency shift measurement correlates with the stress-strain curve for material characterization under tensile test. However, a non-monotonic stiffness variation is observed using the frequency measurement from the polymer

behaviour, which evantually highlights a new investigation trend for fracture behaviour of materials.

## References


[1] K. Goebbels, *Materials Characterization for Process Control and Product Conformity.* (CRC Press, ISBN 0849389577, 1994)

[2] Mfoumou, E.M., Hedberg, C., and Kao-Walter, S., *Vibration-Based Damage Detection and Evaluation of Sheet Materials using a Remote Acoustic Excitation*, submitted for publication, 2006.

[3] Doebling, S.W., Farrar, C.R., and Prime, M.B., *Nondestructive Methods for Materials Characterization*, Proceedings Published as Volume 591 of the Materials Research Society, Symposium Proceedings Series, Provincetown/Orleans, 1999.

[4] Landau L.D., and Lifshitz E.M., *Theory of Elasticity*, 3rd Edition, Pergamon, 1979.

# Paper D

# Static versus Low Frequency Dynamic Elastic Modulus Measurement of Thin Films

**Paper D is accepted in the journal *Technical Acoustics* for publication as:**

Mfoumou, E., Rudenko, O.V., Hedberg, C., and Kao-Walter, S., “Static versus Low Frequency Dynamic Elastic Modulus Measurement of Thin Films”, 2006.

# Static versus Low Frequency Dynamic Elastic Modulus Measurement of Thin Films

Mfoumou, E., Rudenko, O., Hedberg, C. and Kao-Walter, S.

**Abstract**

Understanding the change in material properties in time is necessary for in service diagnosis of structures and prevention of accidents. Therefore, a new experimental technique for evaluating Young's (or elastic) modulus of a vibrating thin film from a dynamic measurement is presented. The technique utilizes bending resonance from a remote acoustic excitation to determine Young's modulus. Equations relating the natural frequencies to the mechanical properties are obtained, and Young's modulus is subsequently determined. Young's modulus values from dynamic test are compared with those (static) obtained by a standard tensile test, from which the procedure and specimen used are according to ASTM-D882 standards for thin plastic sheeting, and consistent results are obtained. The proposed technique is relatively simple and could be used to determine Young's modulus of a wide variety of sheet materials initially having no bending stiffness. It can also be used in service for damage evolution monitoring. Young's modulus is also essential for determining other mechanical properties, such as compliance methods in connections with fracture mechanical testing, fatigue and damage measurements. Moreover, this work emphasizes the feasibility of a damage assessment of components in-service by evaluating changes in the material characteristics.

*Keywords: Tensile test, Young's modulus, film, resonance frequency, nondestructive testing.*

## 1 Introduction

Thin films are used in a wide variety of applications including packaging materials, heat shrink wrap, consumer plastic bags, and adhesive tapes. The purpose of using them may require high stretching like in food wraps, or low stretching such as for protective coatings. Therefore, elastic modulus, which is the measure of the film's resistance to stretching, appears to be an important property to assess.

The films investigated in this study are Low Density PolyEthylene (LDPE) and Paperboard (PPR) of thicknesses $27\mu m$ and $100\mu m$ respectively, shown in figure 1.

Figure 1: Materials studied.

The film is considered as a membrane. Membrane structures are thin three-dimensional surfaces providing significant load resistance only in the direction tangential to their surface. In an ideal case, membrane structures are two-dimensional surfaces having no bending stiffness because they have negligible thickness. In the present study, the material is slightly loaded in the longitudinal direction in order to act as a structural material, and thus can be seen as a membrane with small but non-negligible bending stiffness.

Various testing techniques to determine the properties of thin films have been investigated in literature. In a previous work [1], mechanical and fracture properties of typical thin films were studied by the most common technique which is the tensile test. That technique considers a specimen size according to the standard ASTM-D882 [2]. Among other most established techniques, we can cite the Nano-indentation test [3], especially of thin films on substrates, which determines closed-form relations of Young's modulus $E$ in terms of film thickness and properties of the constituent materials. Shu-Lin Bai [4] also used the nano-indentation technique to determine Young's modulus of thin polymer composites. Bulge or membrane test [5] requires the model of the behavior of the test structure and, in the case of a linear material, can provide Young's modulus; by this test, a membrane of a thin film is prepared by etching away a portion of the substrate on which the film is deposited; the membrane is then pressurized and the measured deflection is used to determine the mechanical properties. Micro-tensile test [6] benefits from its direct measurement of force and displacement. Each of these methods do have strengths and weaknesses with respect to test specimen preparation and experimental result analysis.

Nevertheless, wave propagation characteristics of elastic materials are used extensively for the determination of material properties. Indeed, various techniques for estimation of Young's modulus of a material using its dynamical response have been proposed in literature. Most of the techniques are applicable to bulk materials and those dealing with the investigation of transverse flexural mode use an impact excitation, and a piezoelectric accelerometer contact transducer [7].

More recent approaches based on non-contact excitation and sensing have been developed for measuring mechanical properties. Among these methods, the cantilever beam loading method, in which the load is applied by various means, has become an effective technique. Comella and Scanlon [8] determined the stiffness and elastic modulus of an array of aluminum cantilever beams that were deflected by Atomic Force Microscopy (AFM). Hogmoen et al. [9], and Kang et al. [10] used the optical method to measure the resonance frequency of a cantilever beam to determine its elastic modulus. Kisoo et al. [11] proposed an elastic modulus evaluation technique of a cantilever beam by vibration analysis based on time-average electronic speckle pattern interferometry (TA-ESPI) and Euler-Bernoulli equation. Knowing that elastic material properties critically affect the vibration behavior of structures, Kisoo applied the reverse of this idea, in which the vibration behavior of a particular material can give the elastic properties of the material. The principle is the foundation of all vibration-based identification methods which use the Euler-Bernoulli beam theory to link Young's modulus with the natural frequency of the specimen. Thus, the elastic modulus of a test material can be readily estimated from the measured resonance frequency and Euler-Bernoulli equation. Using the same principle, this paper suggests a technique of vibration-based estimation of Young's modulus of thin films of non-structural materials by the use of the theory of membranes. The suggested technique estimates Young's modulus of thin films by only measuring the strain and the resonance frequency of the material, and outlines the applicability of vibration analysis for material characterization.

## 2 Material Properties and methodology

Material properties play a major role in the mechanical behavior of structures and the properties have been standardized with previous testing methods such as the tensile test and bending test. However, the material properties of thin film may not be the same as those of bulk materials. Thus, it is important to determine the mechanical properties of thin materials to predict the performances of micro structure devices. Because thin films have a thickness of the order of microns, the measurement methods used for bulk materials become inappropriate.

Various material properties like density, Young's and shear modulus, can be found in literature. However, while density and geometric measures generally portray the real values, this may not automatically apply for the specification of Young's or shear modulus. Since the elastic properties are used for dimensioning tasks, the values that are specified by material manufacturers or claimed in customer material standards often can be regarded as rough estimation quantities. Especially thin films with a nonlinear stress-strain relation generally show a wider spreading of the elastic properties compared to homogenous bulk materials, thus the mechanical properties of thin films may have large difference in them due to variations in processing conditions. Indeed, the temperature, humidity, method of etching (if any), or the order of fabrication procedures may induce a great difference in the parameters governing properties.

The vibration measurement is the approach used in this study for extracting the mechanical properties of the material. Vibration measurements are made for a variety of reasons including the verification of an analytical model of a system, and the determination of the resonance frequencies for a system. Resonance frequencies are extremely important in predicting and understanding the dynamic behaviour of a system, but also (during the last decades) in non-destructive estimation of the material mechanical properties.

In many cases, systems are idealized as point masses, rigid bodies, or deformable members without mass, having a finite number of degrees of freedom, inducing a discretization of an analytical model. However, it is also possible to treat systems more rigorously, without discretization of the analytical model. In this study, we analyze a thin film, considered as an elastic body in which the mass and deformation properties are continuously distributed. Because its mass is distributed, an elastic body has an infinite number of natural modes of vibration; as such, its dynamic response may be calculated as the sum of an infinite number of normal-mode contributions. Therefore, the geometry of the specimen will be appropriately chosen (with reduced width for example) in order to involve as few as possible of the normal-modes in the width direction.

The sample under investigation is considered a true membrane, so that the structure satisfies the following conditions:

- The boundaries are free from transverse shear forces and moments in planes tangent to the middle surface.

- The normal displacements and rotations at two parallel edges are unconstrained: that is, these edges can displace freely in the direction of the normal to the middle surface.

- The material has a smoothly varying, continuous surface.

- The components of the surface and edge loads must also be smooth and continuous functions of the coordinates.

These assumptions lead to the two (related) following characterizations of a membrane:

- The material does not have any flexural rigidity, and therefore cannot resist any bending load. As a consequence, although we investigate transverse vibrations, we will not take into account the magnitude of the deflection in the estimation of Young's modulus.

- The material can only sustain tensile loads, which is a key requirement in the derivation of the wave speed from which the resonance frequencies are obtained, leading (in turn) to the estimation of Young's modulus from dynamic mesurement.

In this study, we assume that the material is homogeneous and isotropic, and that it follows Hooke's law. Displacements are assumed to be sufficiently small that the response to dynamic excitations is always linearly elastic. The tensile force in the film is assumed to remain constant during small vibrations in the plane of the film.

# 3 Theory

## 3.1 Governing equation and steady-state vibrations

The equation governing the small-amplitude motion of a thin rectangular specimen is well established in membrane theory. The structure under investigation, with the profile shown on figure 2a, consists of a slightly stretched membrane (having no flexural stiffness) that is free to vibrate transversely. The tensile force F is assumed to remain constant during small vibrations in the y-z plane. In general, vibration of taut membrane which lies in the plane of Cartesian coordinate system and having intrinsic elasticity is governed by the equation [12]:

$$\frac{\partial^2 \xi}{\partial t^2} - c^2 \left( \frac{\partial^2 \xi}{\partial x^2} + \frac{\partial^2 \xi}{\partial y^2} \right) + d^2 \left( \frac{\partial^2 \xi}{\partial x^2} + \frac{\partial^2 \xi}{\partial y^2} \right)^2 = \frac{p\,(x, y, t)}{\rho h} \tag{1}$$

Here $\xi$ is the displacement of membrane along the z - axis from its equilibrium position z=0, $c = \sqrt{T/(\rho h)}$ is the velocity of propagation of bending wave at zero intrinsic elasticity, which is determined by the tensile force $T$ per unit length of

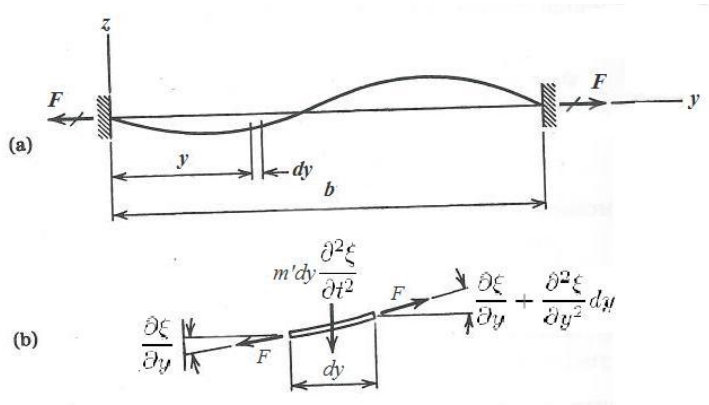


Figure 2: Free body diagram

boundary of membrane, $\rho$ is the density and $h$ is the thickness of the membrane. The external pressure $p(x, y, t)$ is a function of time and of spatial coordinates. $d^2 = \frac{Eh^2}{12\rho(1-\nu^2)}$ where $E$ is Young's modulus and $\nu$ is Poisson's ratio.

Figure 2b shows a free-body diagram of a typical segment of length $dy$, for which the forces in the deformation direction ($z$)are of primary interest. It appears that during free vibrations, the inertia force is counteracted by the difference between the $z$ components of the tensile forces at the ends of the segment.

For a free vibration of the membrane, if the relative contribution of the intrinsic elasticity is small in comparison with the tensile elasticity, it was shown [13] that the solution to equation (1) can be written as a sum of the membrane modes:

$$\xi = \sum_{m,n=0}^{\infty} \xi_{mn} = \sum_{m,n=0}^{\infty} A_{mn} \cos\left(m\pi\frac{x}{a}\right) \sin\left(n\pi\frac{y}{b}\right) \sin\left(\omega_{mn}t + \varphi_{mn}\right). \qquad (2)$$

Here the constants $A_{mn}, \varphi_{mn}$ are amplitude and phase, $\omega_{mn}$ is the natural frequency of mode $mn$.

By substituting (2) into (1), the approximate expressions for natural frequencies are found:

$$\omega_{mn} = c\sqrt{\left(\frac{\pi m}{a}\right)^2 + \left(\frac{\pi n}{b}\right)^2}\left\{1 + \frac{d^2}{2c^2}\left[\left(\frac{\pi m}{a}\right)^2 + \left(\frac{\pi n}{b}\right)^2\right]\right\}, \qquad (3)$$

$m$=0,1,2,3,..., $n$=1,2,3,..., and $a, b$ are the dimensions of the membrane. Each mode in the solution (2) satisfies the boundary conditions

$$\xi_{mn}(x, y = 0) = 0, \quad \xi_{mn}(x, y = b) = 0, \quad \frac{d\xi}{dx}(x = 0, y) = 0, \quad \frac{d\xi}{dx}(x = a, y) = 0. \qquad (4)$$

The conditions (4) correspond to the immovable boundaries at $y = 0, y = b$ and to the free boundaries at $x = 0, x = a$.

The formula (3) is valid for thin films if the second term in the brackets is smaller than unity, condition which can be rewritten as:

$$\delta = \frac{\pi^2}{24}\frac{Eh^3}{(1-\nu^2)Ta^2} << 1. \tag{5}$$

For a standard aluminium foil loaded at $F = 5N$ assuming its Young's modulus to be $70GPa$, the expression (5) leads to the trend given in figure 3. The figure also presents the trend for LDPE with Young's modulus around $150MPa$ having a width of $a = 15mm$ and loaded at $F = 1N$, and for paperboard of same size having Young's modulus of $7GPa$. It appears that the intrinsic elasticity can be neglected up to a thickness of $100\mu m$ for the polymer and paperboard, and roughly $50\mu m$ for aluminium foil, justifying the expression used for Young's modulus extraction in the next section.

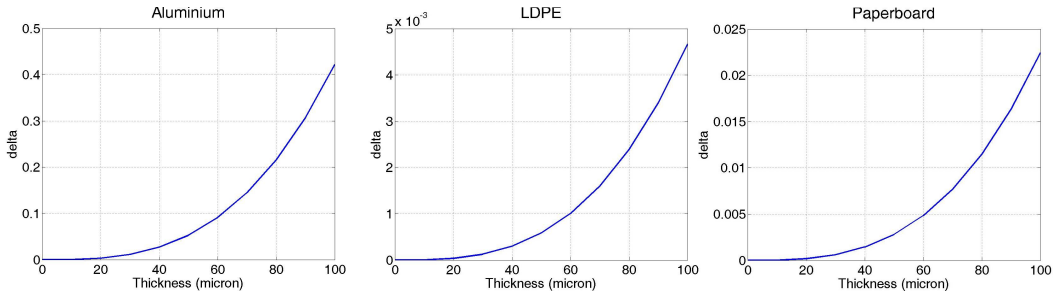


Figure 3: Estimated frequency shift versus thickness variation: account of intrinsic elasticity.

### 3.2 Estimation of Dynamic Young's modulus

A variety of dynamic modulus measurement methods exists including ultrasonic wave propagation and the flexural resonance method presented here for which normal modes of vibration are monitored. In an oscillating system, normal modes are special solutions where all the parts of the system are oscillating with the same frequency (called normal frequencies or allowed frequencies). At resonance from equation (3) neglecting the intrinsic elasticity, and knowing that $c = \sqrt{T/(\rho h)} = \sqrt{\frac{E\cdot\epsilon}{\rho}}$, $\epsilon$ being the strain, it follows that:

$$\omega_{mn} = 2\pi f_{mn} = \sqrt{\frac{E\cdot\epsilon}{\rho}}\sqrt{\left(\frac{\pi m}{a}\right)^2 + \left(\frac{\pi n}{b}\right)^2}, \tag{6}$$

where $m$=0,1,2,3,... and $n$=1,2,3,...

For $m=0$ (bending modes in the length direction), equation (6) can be rewritten as follows:

$$f_{0n}^2 = \frac{E \cdot n^2}{4 \cdot \rho} \cdot \epsilon \tag{7}$$

For a given mode, $n$ is fixed; $a$ and $b$ are constant dimensional properties of the material for a given specimen; $E$ being in turn a material constant (by definition), it follows from equation (7) that the square of the natural frequency is a linear function of the strain. As a consequence, dynamic Young's modulus $E$ can readily be extracted from the slope of the curve.

# 4 Experiment

## 4.1 Specimens

Rectangular strips of uniform width and thickness such as those defined by ASTM-D882 are used. A wide range of specimen gage lengths is used (100mm to 300 mm). For each specimen, the width and thickness were measured three times with a micrometer to the nearest thousandth of a millimeter. The values were averaged in order to be taken into account in the calculation as well as in the testing software TestWorks4 of the MTS Universal Testing Machine used. The thickness of the test specimens was then $27\mu m$ while the width was 15mm. The materials were first placed in a conditioned room with $23^oC$ and an atmospheric humidity of 50% during at least three days. All specimens have a width of 15mm, and five samples are considered with the lengths 100mm, 150mm, 200mm, 250mm and 300mm.

## 4.2 Experimental setup

Main components in the experimental setup (figure 4) consist of a function generator (Agilent Agilent 33220A/20MHz) **A**, a loudspeaker for remote excitation **B**, a laser Doppler vibrometer (Ometron VS-100) **C**, an oscilloscope (LeCroy LT262/350MHz) **D**, and a tensile test machine (MTS QTest 100) **E**. The function generator provides a 8Vpp sine signal to the loudspeaker. The acoustic field excited by the loudspeaker vibrates the sample. Laser detection of the surface vibrational response of the sample is accomplished with the laser vibrometer. The vibrometer used in this study makes high-fidelity and absolute measurements of surface displacement over a bandwidth of DC-50 kHz. The measured response is monitored by the oscilloscope; this allows the detection of the maximum surface displacement, corresponding to a normal mode, which is related to the mechanical properties of the material.


Figure 4: Experimental arrangement.

The specimen under investigation is rigidly held on the clamps as shown in photo (figure 4). The loudspeaker is placed on the back side of the sample such as to excite transversal vibration of the sample. The laser vibrometer is placed opposite to the loudspeaker, and the laser beam is properly focused on the sample surface. Unlike traditional contact vibration transducers, laser-based vibration transducers, or laser vibrometers, require no physical contact with the test object. Remote, mass-loading-free vibration measurements on contact sensitive specimens such as the ones used in this study are some of the motivations for considering a laser-based vibration transducer as the natural choice. The Doppler Effect is utilised here to measure translational vibrations of a single point on the specimen.

### 4.3 Experimental procedure and results

Using the suggested non-contact excitation and measurement setup, a series of acoustic based non-contact experiments were conducted to study dynamic properties, specifically the elastic modulus of the sample sheet material. The ideal medium being assumed to have no stiffness, the specimen is slightly stretched (at most 1mm) in order to make it a structural element.

An external driving force is remotely and harmonically applied to the membrane by the loudspeaker. In steady state, the membrane then vibrates at the frequency of the driving force. When the driving force is at a normal mode frequency, the energy transmission is efficient, so that the material has the maximum surface displacement and vibrates at its resonance frequency. Since the specimen

geometry is a rectangular membrane of small width (to avoid huge interference with propagating waves in the width direction) resulting to normal modes of vibration, the resonant frequencies are sufficiently far apart to permit the use of the peak-amplitude method to determine the resonant frequencies. This transverse vibration response of the material is monitored at a single point of measurement. For each specimen, four sets of measurements are taken corresponding to the four first normal mode of vibration.

For each mode and for each load case (step), the corresponding normal mode as well as the strain were recorded and dynamic Young's modulus was determined by graphical analysis. For each plot obtained from equation (7), a straight line is fitted and Young's modulus determined from the slope of the curve. The initial regions of the plots were ignored because they were non-sensible experimental artifacts. Young's modulus values for all load steps and for each mode were averaged to determine specific dynamic Young's modulus value for each specimen length.

In parallel, the tensile behaviour of the films was monitored as the films were loaded at a constant strain rate of 5% per minute. At least four specimens were tested for each sample. The strain was calculated as the extension divided by the initial length, while the applied force was divided by the cross-section to obtain stress. The stress was then divided by the strain to yield the elastic modulus, within elastic region as given by equation (8).

$$E = \frac{d\sigma}{d\epsilon} \tag{8}$$

where $d\sigma$ is the incremental stress, and $d\epsilon$ the incremental strain.

The elastic modulus was investigated in MD (Machine Direction) for all specimens. The characteristic tensile curves are shown on figures 5 and 6, and the basic statistics about the central tendency and variability of data from tensile test are summarized in tables 1 and 2 with:

- min: smallest value in the data set;
- max: largest value in the data set;
- mean: average of all the values in the data set;
- std: a value characterizing the amount of variation among the values in the data set;
- range: interval between the lowest and the highest value in the data set.

Dynamic Young's modulus is extracted from the frequency measurement according to equation (7). Dynamic and static Young's modulus are then plotted

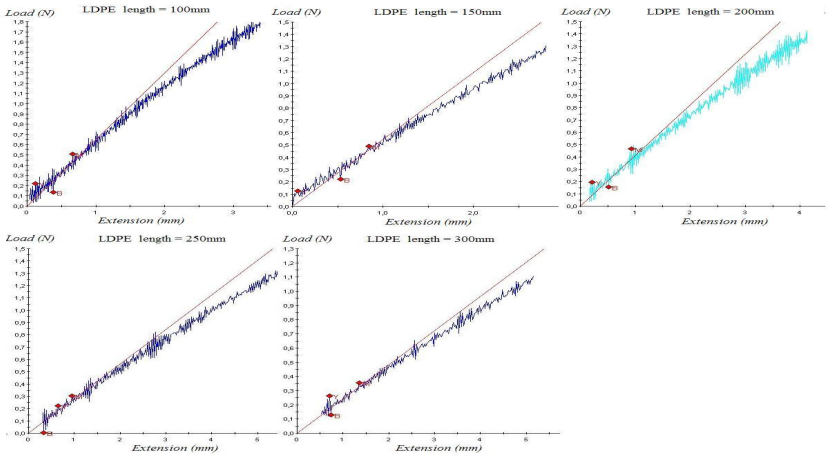


Figure 5: Load vs. extension average plots from tensile test: LDPE.

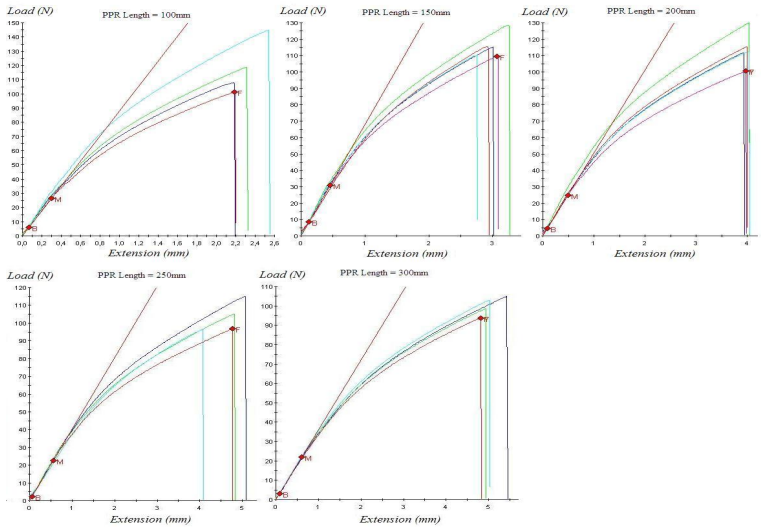


Figure 6: Load vs. extension plots from tensile test: Paperboard.

| Length [mm] | Min [MPa] | Max [MPa] | Mean [MPa] | Std [MPa] | Range |
|---|---|---|---|---|---|
| 100 | 130.2 | 182.9 | 151.5 | 9.75 | 52.74 |
| 150 | 168.4 | 210.5 | 183.4 | 8.86 | 42.16 |
| 200 | 96.09 | 163.3 | 132.1 | 12.7 | 67.11 |
| 250 | 137.7 | 183.1 | 161.1 | 11.69 | 45.43 |
| 300 | 144.1 | 244.9 | 196.4 | 17.29 | 100.8 |

Table 1: Young's modulus obtained from tensile testing: LDPE.

together for comparison for each mode as a function of the specimen length, and presented in figures 7 and 8.

# 5 Discussion

The discrepancies between the dynamic and static results may be due to the following reason: in the dynamic measurements, Young's modulus is obtained from the dynamic behaviour of the specimen and therefore, reflects the frequency dependence of the material. Moreover, the difference of deformation mechanisms may also explain different modulii: the specimen is extended in tensile test, while it is submitted to bending in vibration analysis. Such a difference was explained in a previous work [14] applied to steel, by the fact that certain internal mechanical motions, which lead to a portion of the observed strain, take a fine time to occur. Hence, if there is not enough time during the application of the dynamic (oscillating) force for the strain to occur, the overall strain appears smaller in that case and hence the modulus from the dynamic method becomes higher than the static one. Meanwhile, the Young's modulus of the materials studied in this paper cannot actually be compared with those mentioned in the literature. In fact, Young's modulus values obtained for thin films usually do depend on the constitution and manufacturing process of the material. However, the values of Young's modulus in the present study are in the acceptable range of the values generally obtained, while being lower than those obtained by standard (static) methods. This difference between static and dynamic Young's modulus can be seen on figures 7 and 8 and tables 3 and 4. The extracted values of Young's modulus are found to be between 4.7-6.2GPa for PPR and between 80-127MPa for LDPE, for suitable specimen lengths between 200-300mm and 150-250mm respectively, within which the results are not appreciably affected.

The literature reports the estimation of dynamic Young's modulus, but only for bulk materials, showing that it is higher than static Young's modulus [14-17]. The current work is the first investigation of the estimation of Young's modulus using a dynamic method with a remote acoustic excitation, applied to thin films, showing , in opposition to bulk materials, that the result from the dynamic method is slightly lower than the one from static method. Young's modulii from dynamic method found for each sample length are normalized by the corresponding static values and it follows from figure 9 that the normalized dynamic Young's modulii of both paperboard and LDPE are 70 to 75% of the tensile test values, for specimen lengths between 150 and 250mm. Their difference could not be measured accurately because of the dispersion observed on the data, which is caused by the

| Length [mm] | Min [GPa] | Max [GPa] | Mean [GPa] | Std [GPa] | Range |
|---|---|---|---|---|---|
| 100 | 5.870 | 6.966 | 6.447 | 0.455 | 1.096 |
| 150 | 6.378 | 7.544 | 7.017 | 0.449 | 1.166 |
| 200 | 6.737 | 8.187 | 7.169 | 0.583 | 1.450 |
| 250 | 6.296 | 7.100 | 6.769 | 0.353 | 0.804 |
| 300 | 7.016 | 7.386 | 7.208 | 0.353 | 0.370 |

Table 2: Young's modulus obtained from tensile testing: Paperboard.

| Length [mm] | 100 | 150 | 200 | 250 | 300 |
|---|---|---|---|---|---|
| TT [GPa] | 6.447 | 7.017 | 7.169 | 6.769 | 7.208 |
| Mode 1 | 3.0909 | 4.9649 | 4.7949 | 4.7884 | 5.590 |
| Diff [%] | 52.05 | 29.24 | 33.11 | 29.25 | 22.44 |
| Mode 2 | 3.6808 | 5.5167 | 5.3336 | 5.4020 | 5.0362 |
| Diff [%] | 42.90 | 21.38 | 25.60 | 20.19 | 30.13 |
| Mode 3 | 4.8277 | 3.0891 | 5.2392 | 5.2668 | 6.1915 |
| Diff [%] | 25.11 | 55.97 | 26.91 | 22.19 | 14.10 |
| Mode 4 | 3.1297 | 4.0844 | 4.8651 | 5.2092 | 6.1938 |
| Diff [%] | 51.45 | 41.79 | 32.13 | 23.04 | 14.07 |

Table 3: Comparison of static and dynamic Young's modulus: Paperboard.

| Length [mm] | 100 | 150 | 200 | 250 | 300 |
|---|---|---|---|---|---|
| TT [MPa] | 151.5 | 183.4 | 132.1 | 161.1 | 196.4 |
| Mode 1 | 80 | 127.3 | 115.42 | 123 | 57.7 |
| Diff [%] | 47.19 | 30.58 | 12.62 | 23.64 | 70.62 |
| Mode 2 | 77.17 | 80.6 | 91.52 | 81.7 | 55.2 |
| Diff [%] | 49.06 | 56.05 | 30.71 | 49.28 | 71.89 |
| Mode 3 | 78.44 | 82.8 | 93.88 | 83.6 | 78.2 |
| Diff [%] | 48.22 | 54.85 | 28.93 | 48.10 | 60.18 |
| Mode 4 | 93.27 | 84.1 | 107.45 | 63.8 | 59.7 |
| Diff [%] | 33.43 | 54.14 | 18.66 | 60.39 | 69.60 |

Table 4: Comparison of static and dynamic Young's modulus: LDPE.

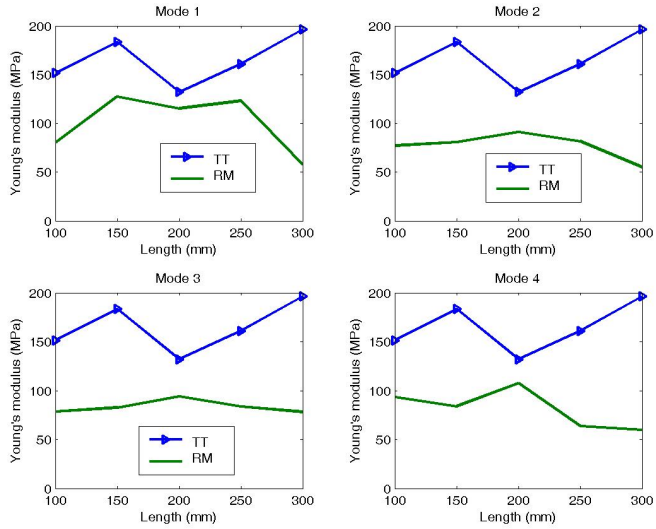


Figure 7: Young's modulus from Static and dynamic methods for LDPE. TT=Tensile Test, RM=Resonance Method.

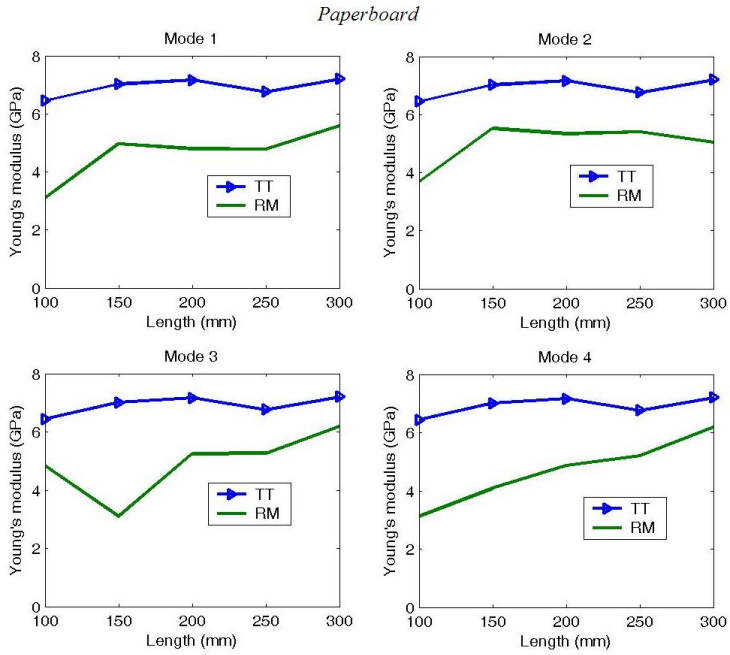


Figure 8: Young's modulus from Static and dynamic methods for Paperboard. TT=Tensile Test, RM=Resonance Method.

extreme sensitivity of the frequency measurement to any inhomogeneity within the material. These residual strain and stress may appear in structures in service because of fatigue loading, or from a combination of mismatched thermal expansion coefficients and intermolecular forces.

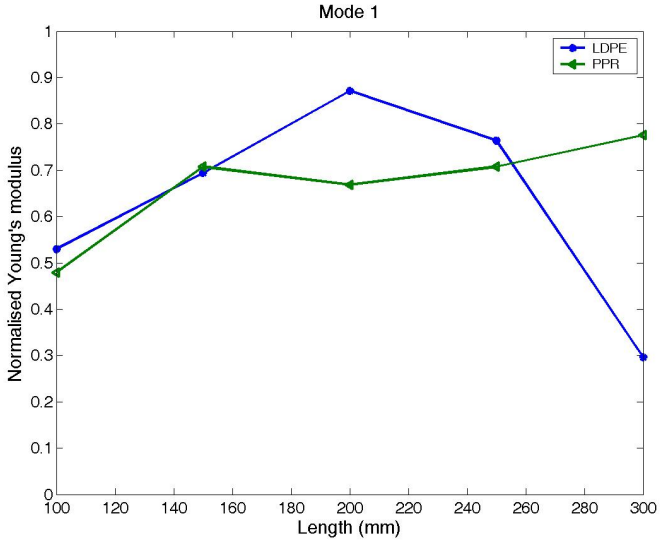


Figure 9: Normalized Young's modulus.

The acoustic method presented in this study has several good features. It is non-destructive, easy to perform, and allows repeated measurements to be made on one specimen. It can be used to characterize a wide range of flat materials. More importantly, it gives a reliable result that can be assured during testing as it has been repeated until the same values, or those within 5% of each other, were obtained at least three times consecutively. Meanwhile, the accuracy of the measurement is strongly dependent on the suitability of the specimen shape and size required. Therefore, flat rectangular specimens must be considered. In addition, specimens must be clamped in a way to display a preload of 0.1 to $0.2N$, as the toe compensation may have a significant influence on the results. The toe region is an artifact caused by a take-off of slack, and alignment or seating of the specimen; it does not represent a property of the material. Therefore, because the $E$ value is directly related to the strain as shown in equation (6), an erroneous estimation of the strain has a direct influence on the slope of the curve and in turn, on the $E$ value.

A deviation is observed from one specimen length to another on the dynamic measurement of Young's modulus. This might come from the fact that the modes are not pure bending along the length of the specimen, which has not been

accounted in the derivation of the equations used. Although this limitation, the current results allow to consider the suggested method as an alternative for the purpose of structural health monitoring of materials of specific sizes. The stiffness of the material changes with introduction of a defect, which can be monitored at a certain interval of time. Therefore, Young's modulus being estimated from natural frequencies, the method confirms the use of the latter for defect detection as already mentioned in a previous work [18].

# 6 Conclusions

Young's modulus is an extremely important parameter to the fracturing process, and also for having a direct relationship to any kind of variation in the structural integrity of the inspected material. Although this material property can easily be measured in the laboratory, it is recommended to be able to assess its changes for use in structures in-situ for the purpose of condition monitoring.

A new non-destructive method for estimation of Young's modulus of thin films from dynamic measurements is therefore presented. This method, based on membrane resonance, uses a non-contacting laser vibrometer system. The non-contacting response measurements, single point measurement, low and high frequency capabilities, and large area coverage are among the advantages of this method.

It is shown that the resonance frequency measurement of thin films in flexural mode is very sensitive to the estimation of the stiffness of the material for a displacement (stretching) as small as $1mm$; this makes the presented method extremely challenging because such sensitivity cannot be expected from standard tensile testing on specimens of the size investigated in this study.

Proper selection of the testing vibrational mode appears important in the suggested method in order to avoid dispersive results (observed on longer and shorter specimen lengths). The dynamic method has the advantage of being simple to set up, however the issue regarding the relevance of dynamic versus static measurements has not been fully addressed. Meanwhile, this work provides the basics for the possibility of remotely predicting damage evolution of structures in service, caused by a residual strain (as small as 0.3%) or stress, a crack, or a local or global weakness of the material. The method can also be applied for evaluation of the effect of water absorption of paper-based sheet materials. Consequently, one can expect the sensitivity of this method to be acceptable for nondestructive testing of sheet materials.

## Acknowledgement

This work was supported by the School of Engineering at Blekinge Institute of Technology. The authors gratefully acknowledge valuable discussions with PhD student Kristian Haller from the same institution, and Professor Shu-Lin Bai, Director of the Centre for Advanced Composite Materials of Peking University, China.

## References

[1] Kao-Walter, S., *On the Fracture of Thin Laminates*, Doctoral Dissertation Series No 2004:07, ISSN 1650-2159, ISBN 91-7295-048-X Blekinge Institute of Technology, Sweden.

[2] ASTM D-882-91, *Standard Test Method for Tensile Properties of Thin Plastic Sheeting.* American Society for Testing and Materials, Philadelphia, Pa., 1991.

[3] Inman, D.J. *Engineering Vibration.*, (Prentice-Hall Inc., NewYork, 1994).

[4] Bai, S., L., *Indentation Properties of the Filler and Matrix in Polymer Composites*, Journal of Materials Science Letters **21**, 2002, 85-88.

[5] Cloud, G., L., *Optical Methods of Engineering Analysis*, (Cambridge University Press, London, 1990)

[6] Hsin-Chang Tsai, Weileun Fang, *Determining the Poisson's ratio of thin film materials using resonant method", Sensor and Actuators A, 103, 377-383 (2003)* , Anal. Chem., 36 (9), 1735-1739, 1964.

[7] ASTM C 1548-02, *Standard Test Method for Dynamic Young's Modulus; Shear Modulus, and Poisson's Ratio of Refractory Materials by Impulse Excitation of Vibration*, ASTM International.

[8] B.T. Comella, M.R. Scanlon, *The determination of the elastic modulus of a microcantilever beam using atomic force microscopy*, J. Mater. Sci., 35, 567-572 (2000).

[9] K. Hogmoen, O.J. Lokberg, *Detection and measurement of small vibration using electronic speckle pattern interferometry* , Applied Optics, 16, 1869-1875 (1977).

[10] Xin Kang, C.J. Tay, C. Quan, *Evaluation of Young's modulus of a vibrating beam by optical method*, Opt. Eng., 42, 10, 3053-3058 (2003).

[11] Kisoo K.; Choi M.; Kim K., *Evaluation of the Young's modulus by resonance frequency and Euler-Bernouilli Equation*, CD-ROM Proceedings of the Thirtheenth International Congress on Sound and Vibration (ICSV13), July 2-6, 2006, Vienna, Austria, Eds.: Eberhardsteiner, J.; Mang, H.A.; Waubke, H., Publisher: Vienna University of Technology, Austria, ISBN: 3-9501554-5-7.

[12] Landau L.D., and Lifshitz E.M., *Theory of Elasticity*, 3rd Edition, Pergamon, 1979.

[13] Mfoumou E.; Hedberg C.; Kao-Walter S., *Vibration-Based Damage Detection and Evaluation of Sheet Materials using a Remote Acoustic Excitation*, submitted for publication, 2006.

[14] Frederick Wilson, A. E. Lord, Jr., *Young's Modulus Determination Via Simple, Inexpensive Static and Dynamic Measurements*, American Journal of Physics, Vol 41, Issue No.1, pp 653-656 (1973).

[15] Turgay .; Kroggel O.; Grbl P., *Propagation of Ultrasound in Concrete - Spatial Distribution and Development of the Young's Modulus*, BB 85-CD International Symposium Non-Destructive Testing in Civil Engineering. Berlin, September 16-19, 2003.

[16] Casper O.; Fabricius Ida L.; Krogsboll A.; Prasad A., *Static and Dynamic Young's Modulus for Lower Cretaceous Chalk. A Low Frequency Scenario.*, AAPG International Conference: October 24-27, 2004; Cancun, Mexico.

[17] *Frac Tips - NSI Technologies, Tulsa/Houston, 1-918-496-2071 - FracTips@nsitech.com*, www.nsitech.com.

[18] Van'kov Yu. V., Kazakov R. B.,Yakovleva E. R., *Natural Frequencies as Diagnostic Criteria for Flaw Detection.*, Electronic Journal "'Technical Acoustics"', http://www.ejta.org, 2003,5.

## ABSTRACT

There is a need to monitor the existence and effects of damage in structural materials. Aircraft components provide a much publicized example, but the need exists in a variety of other structures, such as layered materials used in food packaging industries. While several techniques and models have been proposed for material characterization and condition monitoring of bulk materials, less attention has been devoted to thin sheets having no flexural rigidity. This study is therefore devoted to the development of a new method for acoustic Non-Destructive Testing (NDT) and material characterization of thin sheets used in food packaging materials or similar structures.

A method for assessing the strength in the presence of crack of thin sheets used in food packaging is first presented using a modified Strip Yield Model (SYM). Resonance frequency measurement is then introduced and it is shown, at low frequency range (less than 2kHz), that a change in the physical properties such as a reduction in stiffness resulting from the onset of cracks or loosening of a connection causes detectable changes in the modal properties, specifically the resonance frequency. This observation leads to the implementation of a simple method for damage severity assessment on sheet materials, supported by a new theory illustrating the feasibility of the detection of inhomogeneity in form of added mass, as well as damage severity assessment, using a measurement of the frequency shift. A relationship is then established between the resonance frequency and the material's elastic property, which yields a new modality for sheet materials remote characterization.

The result of this study is the groundwork of a low-frequency vibration-based method with remote acoustic excitation and laser detection, for non-destructive testing and material characterization of sheet materials. The work also enhances the feasibility of the testing and condition monitoring of real structures in their operating environment, rather than laboratory tests of representative structures. The sensitivity of the new experimental approach used is liable to improvement while being high because the frequency measurement is one of the most accurate measurements in physics and metrology.



BLEKINGE TEKNISKA HÖGSKOLA · BTH ·

ISSN 1650-2140

2006:09

ISBN 91-7295-094-3